**ADDIS ABABA UNIVERSITY**
**FACULTY OF TECHNOLOGY**
**SCHOOL OF GRADUATE STUDIES**

# CRACK DETECTION IN A ROTATING DISK

A thesis submitted to the School of Graduate Studies of Addis Ababa University in partial fulfillment of the requirement of the Degree of Masters of Science in Mechanical Engineering
(Applied Mechanics Stream)

Thesis by
Haileleoul Sahle

Advisor
Dr. Alem Bazezew

July 2007


ADDIS ABABA UNIVERSITY

SCHOOL OF GRADUATE STUDIES

DEPARTMENT OF MECHANICAL ENGINEERING

# Crack Detection in a Rotating Disk

Thesis by

Haileleoul Sahle

**Faculty of Technology**

Approved by Board of examiners:

| | |
|---|---|
| Ato Hamsasew Moges | |
| Chairman | Signature |
| Dr. Alem Bazezew | |
| Advisor | Signature |
| Dr. A. Raman | |
| Internal Examiner | Signature |
| Dr. Abiy Aweke | |
| External Examiner | Signature |

## Declaration

This thesis work is my original work and has not been presented for a degree in any other university, and that all source of material are duly acknowledged.

Name: **Haileleoul Sahle**

Title of the Thesis: CRACK DETECTION IN A ROTATING DISK

Department: Hamsalew Moges

Signature: _____

Advisor: Abebe Bazezew

Signature: _____

# CONTENTS

# LIST OF FIGURES

# List of Table

## Abstract

The aim of this thesis is to investigate techniques and parameters that could be used to identify crack if it exist in a rotating disk. Many researches discovered formation or propagation of a crack in a rotating disk will cause a catastrophic failure. Thus, health monitoring for a rotating disk due to crack using crack detection techniques will minimize or reduce the failure that probably to occur.

Among few methods of detecting crack components and due to its feasibility of detection of fatigue crack, vibration-based crack detection techniques are applied in this thesis. This method is based on the fact that change of physical properties (stiffness, mass and damping) due to crack that will manifest themselves as changes in component modal parameters (natural frequency, mode shape and modal damping). Thus, monitoring the selected indicator derived from modal parameters helps to distinguish between crack or un-crack existence and its state in the model.

This thesis demonstrates the change of the vibration characteristic of a rotating disk before and after it is exposed to crack. A mathematical modeling for a rotating disk with crack is derived using conservation of energy. That is, the energy gain of the rotating disk due to inertia load is analyzed by modeling the rotating disk as plate. And, the energy release due to crack formation and propagation is added to the system to approximate the mathematical simulation fully. Then, a numerical equation is derived for finite element analysis.

A powerful finite element analysis software ANSYS is used to simulate the numerically derived equations for the models and to find solutions. Besides, the geometric model which simulate the real rotating disk without and with crack are modeled by commercial software SOLIDWORK for its benefit of modeling complex geometry for the rotating disk with different crack models.

The vibration characteristic and physical changes i.e. distribution of deformation and stress of the rotating disk is studied in relation to different crack orientation and a range of inertia loads for the system. As the result obtained, their relationship and output of the rotating disk without and with crack are discussed. And few recommendations are made for the future study.

# Chapter One

## 1 Introduction

### 1.1 Overview of the project

Interest on application of rotating component has increased dramatically in many engineering designs and products such as flywheels, turbo machines, aircraft engines, machine components in power plants, etc. Sudden failures of these structural components are very costly and may also cause catastrophic failure in terms of human life and property damage. Mostly, their failures have been attributed to the existence of cracks and crack-like defects, [ 1, 2 ].

Although, those structural components might be designed or developed with cracks when they are fabricated, crack growth mostly occurs under steady and varying loads. Moreover, crack propagation and development rises due to various–time–dependent processes, such as fatigue, creep and stress corrosions in their operational period. Fatigue crack growth, which is widely encountered as services failure caused by variability of applied loads on the components. Where as, creep crack growth that occurs as a result of the degradation of material ahead of the main crack by time-dependant cavity at elevated temperature and Stress corrosion crack that occurs due to a process involving conjoint corrosion and straining of a metal due to residual or applied stresses are the categories of steady loading crack formation. Besides, stress corrosion crack growth depends upon the combination of alloy and environment condition.

If the crack geometries are kept to grew till it reaches to their critical size i.e. as a result in a transition from the relatively slow crack growth rates to the fast crack propagation rates, the stress intensity which is a function of the geometry of the component including the crack size, will reaches to the allowable fracture toughness value of the material concerned. Thus, to have a long life and safe operation for the components i.e. working condition is in the design range of fracture toughness, monitoring for components health before and along to its operation period is unquestionable. Consequently, detection for the crack on the rotating components is substantial.

## 1.2 Method of Crack Detection

Traditionally, crack or damage detection was achieved through localized point–by–point inspection techniques. Some of such existing crack inspection techniques as published in ASME code [1983] are the visual inspection, the acoustic or ultrasonic sound method, the magnetic field method and radiograph method. These techniques had principal shortcomings such as requiring highly-skilled man power and a need for much inspection periods. Further, for those techniques, "what we get depends on where we check" because of a prior knowledge of the location of crack based on a previous experience, [1].

However, additional techniques for detection and locating a crack or crack-like damages with better efficiency and economical detection methods had been developed recently. Some of the techniques which are related with the objective of the thesis work are:

**1.2.1 Non Destructive Test (NDT):** some of NDT method of detection that have been used widely for detection of crack on rotor systems are:-

i. Eddy current inspection: Eddy current inspection is one of several NDT methods that use the principle of "electromagnetism" as the basis for conducting examinations. Eddy currents are created through a process called electromagnetic induction. When alternating current is applied to the conductor, such as copper wire, a magnetic field develops in and around the conductor. This magnetic field expands as the alternating current rises to maximum and collapses as the current is reduced to zero. If another electrical conductor is brought into the close proximity to this changing magnetic field, current will be induced in this second conductor. Using this alteration of the generated eddy current, crack detection is conducted. Some of the limitations of eddy current inspection include: Surface must be accessible to the probe; skill and training is required for detection; it is more extensive than other techniques; surface finish and roughness may interfere with the detection of the crack; reference standards are needed for setup; and depth of penetration is limited, [ 3].

ii. Neural network and pattern recognition methods: Neural network provides a general, non-linear parameterized mapping between a set of inputs and a set of outputs. Once trained on available sample data, the neural network can recognize and classify the corresponding patterns based on the input-output mapping. Though this signature analysis capacity had great advantage, most of the time it might not be realistic to obtain vibration data-base under various damage (crack) scenarios because of impractical to let real components to experience all kinds of damage. Therefore, to come up to an appropriate judgment using these techniques, a need of data for the healthy and damaged sample state is required, [ 4 ].

iii. Wavelet analysis: The main advantage of using the wavelet transform is its capability to reveal some hidden aspects of the data that other signal analysis techniques fail to detect. When components vibration signals in the time domain are decomposed into multiple signals using wavelet transform, the change due to structural damage such as crack in each sub-signal may manifest remarkable difference so that higher sensitivity to small damage (crack) may be achieved. However, the selection of optical wavelet and some techniques to eliminate the effect of boundary conditions have been improved, [ 5 ].

**1.2.2 Vibration-based crack detection methods**: This method takes a consideration of change in the assigned vibration characteristic of the component for crack detection. The main vibration characteristic that have been used in vibration–based crack detection method such as frequency, mode shapes and damping ratio are used as a model parameters for its analysis. Since it is expected that this modal parameters are related with the physical properties of the component (mass, damping and stiffness), the change in the physical properties due to crack formation or propagation can reveal themselves as change in modal parameters. As a result such modal parameters used as an indicator for crack existence on the component.

In general, there are two approaches which are used in vibration–based crack detection method, [ 1 , 5 ]. These are:

**1.2.2.1** Non-model methods detect damage via the direct use of such quantities as

i. *Frequency change* A common method based on identifying changes in modal frequencies resulting from local stiffness changes or mass loss. Care should be given for measuring and processing errors using this techniques or it should be coupled with other localization damage detection method like mode shapes.

ii. *Mode shapes* mostly used in conjunction with natural frequencies. Deterioration of a structure can alter local stiffness and cause discontinuity near regions. The consequent change of mode shapes depends on both the severity and the location of the damage where crack occurs. The magnitude of change with respect to each mode may vary from one to another. This can be used as a tool to predict the location of the crack.

iii. *Damping* is normally expected in a cracked component that would increase the damping over the un-cracked components because of the friction between cracked surfaces. However, for crack detection, it is less likely to choose damping as an indicator compared to natural frequencies and mode shapes. One of the reasons is the lack of accuracy in determining damping ratios. There are situations where damping may be the preferable indicator when frequencies and mode shapes are insensitive to crack, [ 6 ].

**1.2.2.2** Model-based methods use a pre-selected set of parameters to define the model of the component under investigation and the assumed damage mechanisms. The damage state of the component is then determined by means of changes in the values of these parameters relating to the model. Typically, finite element models are often used in such occasions. Two steps which are often involved in the crack detection process are to produce a validated finite element model of the undamaged state as a baseline and to renew the model to obtain a model in damaged state matching the measured vibration data at the damaged state. Comparison of the updated values to the baseline model

provides an indication of the damage and can be used to quantify the location and extent of damage. Determination of very accurate mathematical model that correctly captures the actual components dynamic behavior in some predetermined frequency range is necessary. Hence, this approach seems more effective to simple components than complex components,[ 7 ].

Taking into account the above discussion, a vibration-based crack detection approaches is preferred and applied for the thesis work. Further supportive advantages of vibration-based detection with NDT and traditionally used crack detection approaches are, the modal parameterizes for characterizing the vibrating components include both global and local information of the components dynamic properties; the global nature of the parameters (such as natural frequencies and mode shapes) implies that tests can be conducted at virtually arbitrary points; a prior knowledge of the damage location is not necessary; hidden damage, which is normally difficult to access, can be detected by this approach; the availability of high-speed portable computers and data acquisition systems has made it feasible to integrate vibration monitoring into the routine maintenance program at a relatively low cost. Besides, we can also take its advantage that is the applicability does not depend on the structural material in use, which means that it can be used for non-metallic or composite structures.

### 1.3 Objective of the thesis

The general objective of this thesis is to develop methods of detection of crack in a rotating disk using analytical simulations. And if an experimental set ups available, verification on the analytic simulation result will be verified.

The Specific Objectives of the thesis include

i. Modeling a solid rotating disk.
ii. Modeling a notch on the rotating disk as one types of crack
iii. To find qualitative change of parameters those manifest themselves for crack detection on the rotating disk.

These objectives will be achieved by employing the following procedures:

- Modeling a solid rotating disk with a structural member.

- Modeling the crack on the solid rotating disk in terms of the type of crack on position where crack propagate on the real physical components.
- Appling finite element analysis to describe the crack influence on the selected modal parameters and component physical properties [stiffness, mass and damping].
- Discussion on the result of the analysis, in terms of the difference between rotating disk without and with crack.
- Discussion on the parameter that identify a crack on a rotating disk for detection purpose.

# Chapter Two

## 2 Literature Review

### 2.1 Introduction

Health monitoring and online crack detection are increasingly gaining the interest of rotating component designers and manufacturers for benefit of safe operation and a need for lower maintenance costs. However, the research out puts on this area is limited. Some of the researches' out put in relation to the objective of this thesis are:

### 2.2 On Rotating Disk

Jintai C., et al, [ 8 ] derived the governing equation for free vibration of a spinning circular disk by using the variational formulation based upon the Kirchhoff plate and von-Karman strain theory. They demonstrated that, the derivation of the governing equation, which was theoretically valid under the assumption of in-plane deflections, is steady and axisymmetric. They conduct analysis for natural frequency and critical speeds for a freely spinning disk. Further they illustrate the dependencies of spinning speed, mode number and natural frequency with natural frequency for stationary disk,.

J. Chung, et al, [ 9 ] also analyzed non-linear dynamic responses for a flexible spinning disc with angular acceleration based on the Kirchhoff plate theory and the von-Karman Strain theory. Their derived non-linear equations of motion are coupled of the radial, tangential and transverse displacements equations. Their analysis results shows the natural frequencies for the radial and tangential motion are higher than those of the transverse motion. The radial and tangential displacements have relatively higher frequency components compared to the transverse displacement and the effects of angular acceleration on the dynamic responses of the system are showed briefly.

Wook H. and Jintai C. , [ 10 ] analyzes the dynamic characteristics and responses of a flexible rotating disk, when the disk has angular misalignment. They derived an equation of motion in the transverse, radial and tangential displacements by applying

von Karman strain theory and the Kirchhoff plate theory. In their work, it is illustrated that equations are fully coupled partial differential equations through the transverse, radial and tangential displacements. Moreover, the equation of transverse motion is non-linear while the others are linear. Finite element method is applied after the non-linear equation is linearized in the neighborhood of a dynamic equilibrium position. The effects of angular misalignment on the natural frequencies, the mode shapes and the dynamic responses are investigated. Moreover, their analysis shows that the angular misalignment causes the natural frequency split and the out-of-plane mode with only one nodal diameter and no nodal circle has the largest frequency split. And the angular misalignment yields the amplitude modulations in the transverse, radial and tangential dynamic responses.

T. Tomioka, et al, [ 11 ] developed an analysis of free vibration of rotating disk-blade coupled systems by using Ritz method. They used artificial spring at the joint of disk and blades for satisfying the boundary conditions and continuity condition. And, for numerical analysis, an Orthogonal polynomials generated by the Gram-Schmidt process were used as the admissible functions. Their final out put shows that, the disk-blade coupled vibration occurs when some specific relations between the number of blades and the nodal diameter components of the disk are satisfied.

**2.3 On Crack Characteristic on a Rotating Disk**

Wen-hwa and Ta-chyan , [ 12 ] they conduct analysis of crack based on a modified Hamilton's principle for fast rotating disks with mixed-mode cracks. They derived a finite element model such that the proper crack-tip singularities to be considered and the inter-element displacement compatibility conditions as well implemented in their analysis. They determine the mixed-mode stress intensity factors, the modified J-integrals for rotating cracked disks taking into account the effect of centrifugal force. Further, they predict the direction of crack growth of a rotating disk with an arbitrary internal crack using the "strain-energy density factor" concept. For evaluating the integrity of structures, natural vibrations of cracked disk they conduct a Non-destructive Testing. In their research verification, the simple case of a rotating disk

with radial cracks is solved and appreciated correlations between the computed results and reference solution are obtained.

P. Rooke and J. Tweeds, [ 13 ] derived solution for stress intensity factor at both crack tips and a crack formation energy with the help of 'Fredholm equation'. For their elastic analysis, they use a radial crack model in finite rotating elastic disk.

Makoto I. , [ 14 ] uses the 'Eigen function' expansions for determining the complex stress potentials for a rotating disk containing an internal crack at an arbitrary position. While the unknown coefficients in the equations are formulated from, the boundary conditions expressed in terms of the resultant forces. In his study, numerical calculations are done for various configuration and convenient formulae for the stress intensity factors.

M. Lorenzo and J. Cartwright , [ 15 ] determine the strip yield zone length and crack tip opening displacement for an internal radial crack in a rotating annular disk. In their analysis a range of crack lengths and rotational speeds used as input parameters. Their analysis is illustrated by the boundary element method combined with subtraction of 'Bueckner singular fields' to obtain weighting functions. Besides, for their analysis they use a general representation of the weight function, which leads to integrals that can be evaluated analytically to obtain the stress intensity factor and surface displacements of the crack. And the determination of crack tip opening displacements for the strip yield crack is showed to be reduced to a non-singular integral which can be evaluated in closed form.

**2.4 On Detection of a Crack on a Rotor and Rotating Disk**

Xin H., et al ,[ 16 ] to illustrate the presence and growth of cracks, by following a combined computational and experimental study of the vibration characteristics of a composite hub flywheel rotor system with a cracked hub disk. Their experimental test was carried on both in-plane and out-of-plane vibration characteristics. A rotor with a composite disk hub supporting a relatively massive rim used for the experiment whiles a crack that is deliberately introduced into the hub disk during fabrication. In addition, they developed a finite element model for further explore the relationship

between natural frequencies and crack properties. And at last, a simplified theoretical model for the primary in-plane vibration mode was developed and used in a series of parametric studies. As per their study, at final step a good agreement was found between the model predictions and the experimental results. Their observation on the presence of a crack tends to affect both the magnitudes and distribution of the rotor natural frequencies. Primary frequencies for rotors with a crack are smaller than for those without a crack. In addition, they suggest the frequency values of associated with the "in-crack" direction are generally smaller than those associated with the "off-crack" direction, introducing a non-symmetry into the rotordynamics which can serve as an indicator for rotor health monitoring.

Itzhak G. and Cody C., [ 17 ] conduct two theoretical analyses on global and local asymmetry crack models. They utilized to identify characteristics of the system response that may be directly attributed to the presence of a transverse crack in a rotor. Their study result shows, the behavior of the 2X harmonic component of the system response is an effective target observation for monitoring system of introduced of a crack in rotor system. However, the detection of change in the magnitude of the 2X harmonic component of the system response became much more difficult for shaft speeds which are greater than 2X resonance speeds.

Andrew L., et al, [ 18 ] presents the analytical result concerning the detection of a crack in a rotating disk. The concept of their approach is based on the fact the development of a disk crack results in a distorted strain field within the components. As a result, a minute deformation in the disk's geometry as well as a change in the system's center of mass occurs. In their work, they use various notch sizes to simulate an actual crack on a disk for their finite element analysis. Besides, their analytical study results the overall changes in the disk's geometry and center of mass with small magnitude.

A detection of a crack on a rotating disk of a turbine is conducted by a Non Distractive Test (NDT) by the Nondestructive evaluation group at NASA Glenn research center, Lewis Field in Cleveland. Their assessing for feasibility of utilizing

real-time vibration data is obtained from radial blade tip clearance and shaft clearance measurements using capacitive or eddy current probes, [ 4 ].

Wayne C. and Michel J., [ 19 ] develop a system to detect, discriminate and tack fatigue cracks in a rotating disk. Their effort produces a physical –based model that describes the change in the center of mass of a rotating disk using damping ratio, initial unbalance and crack size as parameters. They also developed a method for detecting and discriminating a crack using a single cycle of data. They validated their results through testing in a spin pit detection machine.

### 2.5 Organization of the Thesis

Chapter one, main causes for failure of rotating disk failure (crack) and methods which are familiar with detection of the considerable failure cause is crack are discussed. The review of literatures will be summarized on the second chapter. The analytical and finite element modeling for the rotating disk with basic consideration and assumption of crack discussed in the third and forth chapter respectively. The derivation and solution techniques are presented in chapter fifth. The results obtained and their discussions are included in sixth chapter. Finally conclusion and recommendations for future research are mentioned in the last chapter.

# Chapter Three

## 3 Derivation on Equations of Motion

### 3.1 Introduction

In this study, to determine the governing equation of motion for the rotating disk that exposed to crack in partial differential form, simple approaches are applied. First, a governing equation for the rotating disk without a crack is analyzed considering the rotating disk as a flexible body which will had an energy transformation between Kinetic, potential and strain energy due to its high angular rotation. Then, the effect of crack formation i. e an energy release from the system is added.

### 3.2 Rotating Disk without Crack

One of the best approaches for formulating the equation of motion for a rotating disk is by following Kirchhoff plate theory [ 20,21 ] and Von-Karman strain theory [20,21 ]. This is the most commonly applied method for these classes of problems. Hence it is reported that through the analysis by finite element method a three dimensional elasticity approach is used.

Thus, let's consider a flexible rotating disk fixed to a shaft at its inner radius $r = R_i$ and free at its outer edge i.e. at $r = R_O$. The flexible rotating disk rotates about the rotation axis or the shaft axis Z with a constant angular speed $\Omega$. Consequently, the flexible rotating disk will be under an inertia load (i.e. centrifugal force).

For defining a relation for displacement of the points and load and stress distribution in the flexible rotating disk as well theirs relationship, a cylindrical coordinate system by assigning the reference plane to be the middle surface of the plane element is used.

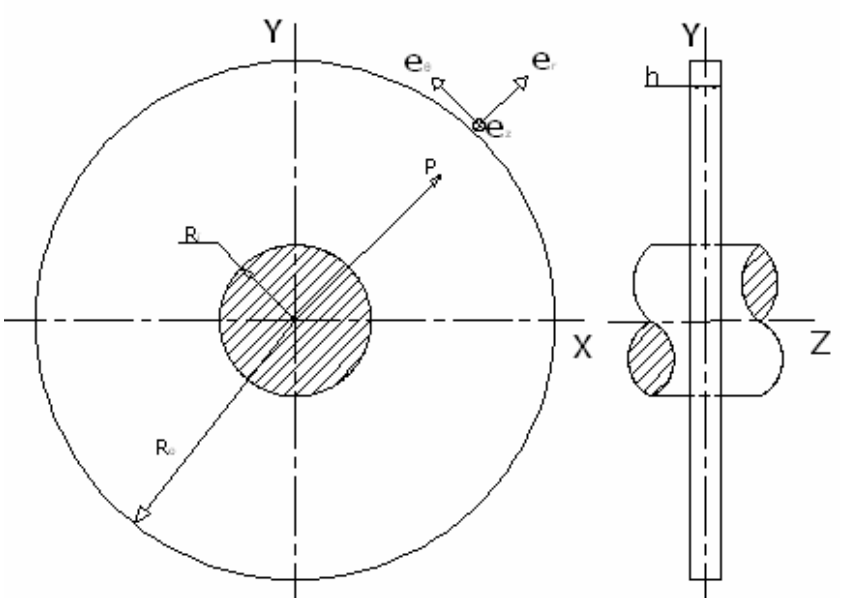


Figure 3.1 Flexible rotating disks

Using a free body diagram for small elemental as described in figure 3.2 for a Point P, its position inside the disk can be defined by the radial co-ordinate r and the tangential co-ordinate θ and the transverse co-ordinate z. Thus, the displacement can be represented by the radial displacement $\mathbf{u}_r$ the tangential displacement $\mathbf{u}_\theta$ and the transverse displacement $\mathbf{u}_z$. Further Using the Kirchhoff plate theory and a free body diagram for the element, these displacements are expressed in terms of the displacements for a point on the middle surface of the disk as

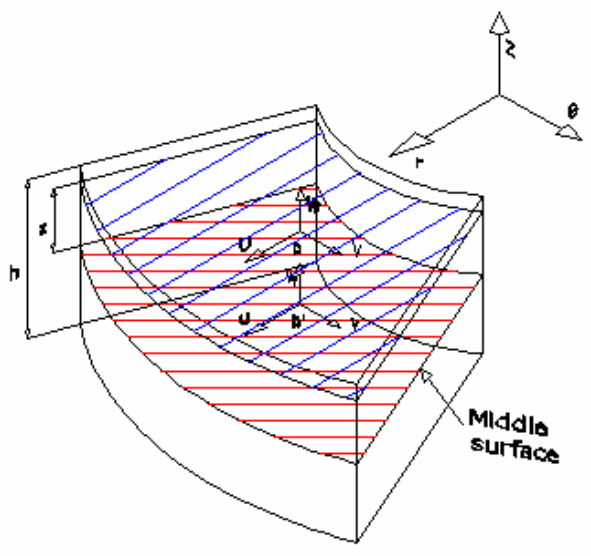


Figure 3.2 An element of a plane with its reference middle surface

$$\begin{aligned} \mathbf{u}_r &= u - z\frac{\partial w}{\partial r} \\ \mathbf{u}_\theta &= v - z\frac{\partial w}{r\partial \theta} \\ \mathbf{u}_z &= w \end{aligned} \tag{3.1}$$

Where: $u(r,\theta,t)$, $v(r,\theta,t)$ and $w(r,\theta,t)$ are the radial, tangential and transverse displacements of a point P' on the middle surface of the disk, respectively.

The stress distributions on an element of the rotating disk are shear stress $\sigma_{r\theta}$ and normal stress $\sigma_{rr}$ & $\sigma_{\theta\theta}$ whose variations are considered to be linear over the thickness,[20] .

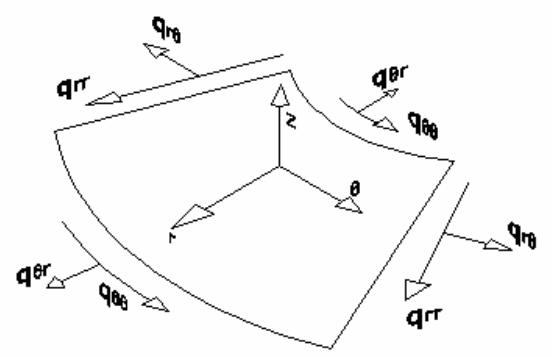


Figure 3.3 Resultant tractions a reference middle surface

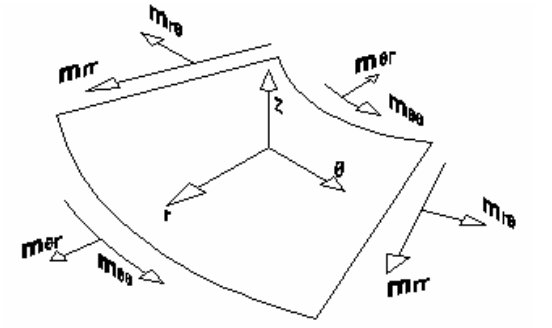


Figure 3.4 Resultant moment on a reference middle surface

The relation of these stresses with the resultant force and moment defined by equation (3.2) and it distribution on the middle surface shown in figure 3.3 and figure 3.4 respectively.

$$q_i = \int_{-h/2}^{h/2} \sigma_i dz \qquad m_i = \int_{-h/2}^{h/2} z\sigma_i dz \tag{3.2}$$

Where: $q_i =$ Forces along $i = r, \theta \, and \, z$

$m_i =$ Moments along $i = r, \theta \, and \, z$

$\sigma_i =$ Stresses and

$z$ is position.

### 3.2.1 Kinetic Energy of the Rotating Disk

To determine the kinetic energy of the flexible rotating disk due to its high angular rotation, let first take point P whose position vector $\vec{r}$ is:

$$\vec{r} = (r + u_r)e_r + u_\theta e_\theta + u_z e_z \tag{3.3}$$

Where $e_r$, $e_\theta$ and $e_z$ are the unit vectors in the r, θ and z directions. And the velocity vector $\vec{V}$ , for which the angular rotation $\vec{w} = \Omega e_z$

$$\vec{V} = V^o - z\psi \tag{3.4}$$

$$V^o = \left(\frac{\partial u}{\partial t} - \Omega v\right)e_r + \left[\frac{\partial v}{\partial t} + \Omega(r+u)\right]e_\theta + \left(\frac{\partial w}{\partial t} + \Omega\frac{\partial w}{\partial \theta}\right)e_z \tag{3.5}$$

$$\psi = \left[\frac{\partial^2 w}{\partial t \partial r} - \Omega\left(\frac{\partial w}{r\partial\theta} - \frac{\partial^2 w}{\partial r \partial \theta}\right)\right]e_r + \left[\frac{\partial^2 w}{r\partial t \partial \theta} + \Omega\left(\frac{\partial w}{\partial r} + \frac{\partial^2 w}{r\partial\theta^2}\right)\right]e_\theta \tag{3.6}$$

where $V^o$ the velocity vector due to in-plane and $\psi$ is the angular velocity vector due to bending about the middle surface.

Thus, Assuming that the disk thickness is small as related with the outer radius, the general kinetic energy expression for the flexible rotating disk can be described as,[ 8 ].

$$T = \frac{1}{2}\rho h \int_A V^o \bullet V^o dA \tag{3.7}$$

where $\rho$ is the mass density of the disk, $h$ is the thickness, and A is the area of flexible rotating disk.

Substituting equation (3.5) in equation (3.7), and after simplification, equation (3.7) yields

$$T = \frac{1}{2}\rho h \int_A \left\langle \left(\frac{\partial u}{\partial t} - \Omega v\right)^2 + \left[\frac{\partial v}{\partial t} + \Omega(r+u)\right]^2 + \left(\frac{\partial w}{\partial t} + \Omega\frac{\partial w}{\partial \theta}\right)^2 \right\rangle dA$$

$$T = \frac{1}{2}\rho h \int_A \left\{ \left[\left(\frac{\partial u}{\partial t}\right)^2 + \left(\frac{\partial v}{\partial t}\right)^2 + \left(\frac{\partial w}{\partial t}\right)^2\right] + \left[(\Omega r)^2 - 2\Omega v\frac{\partial u}{\partial t} + \Omega^2 (r+v)^2\right] \right.$$
$$\left. + \left[2\frac{\partial v}{\partial t}\Omega(r+u) + \left(\Omega\frac{\partial w}{\partial \theta}\right)^2 + 2\Omega\frac{\partial w}{\partial t}\frac{\partial w}{\partial \theta}\right] \right\} dA \qquad (3.8)$$

### 3.2.2 Potential Energy of the Rotating Disk

Considering the flexible rotating disk as an elastic body, the inertia load that is generated due to the angular rotation develops an elastic energy. Hence, this elastic potential energy can be considered to be equal with the strain energy of the system. And, the general strain energy for system can be expressed as, (it may be noted that, the centrifugal field on strain is neglected as first approximating)

$$U = \int_V \left( \int_0^{\varepsilon_{ij}} \sigma_{ij} d\varepsilon_{ij} \right) dV \qquad (3.9)$$

where $\sigma_{ij}$ is stress, $\varepsilon_{ij}$ is strain and $V$ is the volume of the disk. Substitute the constitutive equation for the linear elastic response of isotropic material in equation (3.9), it yields

$$U = \int_V (\frac{\lambda}{2}\varepsilon_{kk}\varepsilon_{jj} + G\varepsilon_{ij}\varepsilon_{ij}) dV \qquad (3.10)$$

Where, Lame's constant: $\lambda = \dfrac{\upsilon E}{(1+\upsilon)(1-2\upsilon)}$

Shear modulus: $G = \dfrac{E}{2(1+\upsilon)}$,

$E$ modules of elasticity and $\upsilon$ is poison's ratio

One dimensional form for equation (3.10) would be

$$U = \frac{1}{2}\int_V (\sigma_{ij}\varepsilon_{ij})dV \tag{3.11}$$

Further considering the variation of stress along Z axis is not varied, equation (3.10) can be expressed as

$$U = \frac{1}{2}\int_V (\sigma_{rr}\varepsilon_{rr} + \sigma_{\theta\theta}\varepsilon_{\theta\theta} + 2\sigma_{r\theta}\varepsilon_{r\theta})dV \tag{3.12}$$

Integrating the term in equation ( 3.12 ) parentheses from $-h/2$ to $h/2$ with respect to Z. The strain energy can be rewritten as

$$U = \frac{1}{2}\int_A \left( \underbrace{q_r\varepsilon_r^o + q_\theta\varepsilon_\theta^o + 2q_{r\theta}\varepsilon_{r\theta}^o}_{Membrane-energy} + \underbrace{m_r k_r + m_\theta k_\theta + 2m_{r\theta}k_{r\theta}}_{bending-energy} \right) dA \tag{3.13}$$

Where A is the area of the flexible rotating disc, $\varepsilon_r^o, \varepsilon_\theta^o and \varepsilon_{r\theta}^o$ are the strains at a point on the middle surface. $k_r$, $k_\theta$ and $k_{r\theta}$ are the curvature changes of the deflected middle surface, i.e. a strain due to bending contribution:

$$k_r = -\frac{\partial^2 w}{\partial r^2}, \quad k_\theta = -\left(\frac{\partial^2 w}{r^2\partial\theta^2} + \frac{\partial w}{r\partial r}\right) \quad k_{r\theta} = -\left(\frac{\partial^2 w}{r\partial r\partial\theta} - \frac{\partial w}{r^2\partial\theta}\right) \tag{3.14}$$

Using Von-Karman strain theory for the consideration of linear and nonlinear terms of strain, $\varepsilon_i = \varepsilon^o - zk_i$ for $i(r,\theta,z)$ strain at middle surface became

$$\varepsilon_r^o = \frac{\partial u}{\partial r} + \frac{1}{2}\left(\frac{\partial w}{\partial r}\right)^2, \qquad \varepsilon_\theta^o = \frac{\partial v}{r\partial\theta} + \frac{u}{r} + \frac{1}{2}\left(\frac{\partial w}{r\partial\vartheta}\right)^2$$

$$\varepsilon_{r\theta}^o = \frac{1}{2}\left(\frac{\partial u}{\partial r} + \frac{\partial v}{\partial r} - \frac{v}{r} + \frac{\partial w}{\partial r}\frac{\partial w}{r\partial\theta}\right) \tag{3.15}$$

And for $q_r$, $q_\theta$ and $q_{r\theta}$ which are the linearized internal forces and $m_r$, $m_\theta$ and $m_{r\theta}$ for linearized moment per unit length of the middle surface expressed as,

$$q_r = D_o\left[\frac{\partial u}{\partial r} + \nu\left(\frac{\partial v}{r\partial\theta} + \frac{u}{r}\right)\right], \qquad q_\theta = D_o\left[\nu\frac{\partial u}{\partial r} + \frac{\partial v}{r\partial\theta} + \frac{u}{r}\right]$$

$$q_{r\theta} = \frac{1-\nu}{2}D_o\left[\frac{\partial u}{r\partial\theta} + \frac{\partial v}{\partial r} - \frac{v}{r}\right] \tag{3.16}$$

$$m_r = -D\left[\frac{\partial^2 w}{\partial r^2} + \frac{v}{r}\left(\frac{\partial w}{r\partial\theta} + \frac{\partial w}{r\partial\theta}\right)\right], \qquad m_\theta = -D\left[\nu\frac{\partial^2 w}{\partial r^2} + \frac{1}{r}\left(\frac{\partial w}{\partial r} + \frac{\partial w}{r\partial\theta}\right)\right]$$

$$m_{r\theta} = -\frac{(1-\nu)}{2}D\left[\frac{\partial^2 w}{\partial r\partial\theta} - \frac{\partial w}{r\partial\theta}\right] \tag{3.17}$$

which $D_0$ and $D$ are the extensible rigidity and flexural rigidity of the flexible rotating disc respectively

$$D_o = \frac{Eh}{1-\nu^2}, \qquad D = \frac{Eh^3}{12(1-\nu^2)} \tag{3.18}$$

If there exists non-conservative forces in the system, the work done by the non-conservative forces expressed as

$$W_{nc} = \int_A (P_r u + P_\theta v + P_z w)dA \tag{3.19}$$

where $P_r, P_\theta$ and $P_z$ are non-conservative forces in the r, θ and z direction, respectively.

Finally, substituting those relations between linearized force and moments as well displacement relation with stress and strain in equation (3.13) and for this system the non-conservative forces are assumed to be zero. (i. e $P_r = P_\theta = P_z = 0$). Thus the total strain energy obtained as

$$U = \frac{1}{2}\int_A \left\{ q_r\left(\frac{\partial u}{\partial r} + \frac{1}{2}\left(\frac{\partial w}{\partial r}\right)^2\right) + q_\theta\left(\frac{\partial v}{r\partial\theta} + \frac{u}{r} + \frac{1}{2}\left(\frac{\partial w}{r\partial\theta}\right)^2\right) + q_{r\theta}\left(\frac{\partial u}{r\partial\theta} + \frac{\partial v}{\partial r} - \frac{v}{r} + \frac{\partial w}{\partial r}\frac{\partial w}{r\partial\theta}\right)\right.$$

$$\left. + (\nabla^2 w)^2 - 2(1-\upsilon)\left(\frac{\partial^2 w}{r\partial r}\left(\frac{\partial w}{r\partial r} + \frac{\partial^2 w}{r^2\partial\theta^2}\right) - \left(\frac{\partial^2 w}{r\partial r\partial\theta} - \frac{\partial w}{r^2\partial\theta}\right)^2\right)\right\} dA \tag{3.20}$$

where

$$\nabla^2 w = \frac{\partial^2 w}{\partial r^2} + \frac{1}{r}\frac{\partial w}{\partial r} + \frac{1}{r^2}\frac{\partial^2 w}{\partial \theta^2} \tag{3.21}$$

The equations of motion and the boundary conditions for a flexible rotating disc can be derived by applying Hamilton's principle, [ 23 ].

The general expression for the Hamilton's Principle between two arbitrary time's $t_1$ and $t_2$ expressed as

$$\int_{t_1}^{t_2} (\delta T - \delta U)dt = 0 \tag{3.22}$$

Where T is the kinetic energy and $U$ is strain and/or potential energy of the system. Substituting equation (3.8) and equation (3.20) for the kinetic energy and strain energy of the system in equation (3.22), equations for the radial, tangential and transverse displacements for the flexible rotating disk without crack are obtained as, [ 8, 9, 10 ].

$$\rho h\left(\frac{\partial^2 u}{\partial t^2} - 2\Omega\frac{\partial v}{\partial t} - \Omega^2 u\right) - \frac{\partial q_r}{\partial r} - \frac{\partial q_{r\theta}}{r\partial\theta} - \frac{q_\theta}{r} = \rho h\Omega^2 r \tag{3.23}$$

$$\rho h\left(\frac{\partial^2 v}{\partial t^2} + 2\Omega\frac{\partial u}{\partial t} - \Omega^2 v\right) - \frac{\partial q_\theta}{r\partial\theta} - \frac{\partial q_{r\theta}}{\partial r} - \frac{q_{r\theta}}{r} = 0 \tag{3.24}$$

$$\left\{\rho h\left(\frac{\partial^2 w}{\partial t^2} + 2\Omega\frac{\partial^2 w}{\partial t\partial\theta} + \Omega^2\frac{\partial^2 w}{\partial\theta^2}\right) + D\nabla^4 w - \frac{\partial}{r\partial r}\left[r\left(q_r\frac{\partial w}{\partial r} + q_{r\theta}\frac{\partial w}{r\partial\theta}\right)\right]\right.$$
$$\left. - \frac{\partial}{r\partial\theta}\left(q_{r\theta}\frac{\partial w}{\partial r} + q_\theta\frac{\partial w}{r\partial\theta}\right)\right\} = 0 \tag{3.25}$$

Where $\nabla^4 = \left(\nabla^2\right)^2$

The corresponding boundary conditions are the same as those of a conventional rotating disk. The boundary conditions are

- Displacement and slope at $r = a : -\ u = 0; v = 0; w = 0; \frac{\partial w}{\partial r} = 0$ (3.26)

- Force and moment at

$$r = b : -q_r = 0; q_{r\theta} = 0; m_r = 0; -D\frac{\partial \nabla^2 w}{\partial r} + \frac{\partial m_{r\theta}}{r\partial \theta} = 0 \tag{3.27}$$

Attention should be given to the above equation. That is equation (3.23) and (3.24) are linear equations while equation (3.25) is a non-linear equation because the linearized forces $q_r, q_\theta \text{ and } q_{r\theta}$ are only a function of $u \text{ and } v$, equation (3.16).

### 3.3 A Rotating Disk with Crack

To determine the governing equation of motion for a flexible rotating disk with a through crack, we have to consider the effect of energy release due to crack formation. Thus the total strain energy for the flexible rotating disk with a crack will be equal to total strain energy of the flexible rotating disk without a crack.

$$U_T = U - U_C \tag{3.28}$$

Where $U_T$ is total strain energy for the flexible rotating disk with through crack.

$U$ is strain energy for the flexible rotating disk without crack.

$U_C$ is loss strain energy due to crack formation on the flexible rotating disk.

#### 3.3.1 Modeling of a Crack

In cracked structures, the stress field near crack-tips may be one of the three modes of fracture as it seen in Figure 3.5. These modes of fractures are categories as

- Mode I (Tension, opening), is associated with local displacement in which the crack surfaces move directly apart.
- Mode II ( In-plane Shear, Sliding), is characterized by displacement in which the cracked surfaces slide over one another perpendicular to the leading edge of the crack.
- Mode III ( out-of-plane-Shear, Tearing ), finds the crack surfaces sliding with respect to one another parallel to the leading edge.

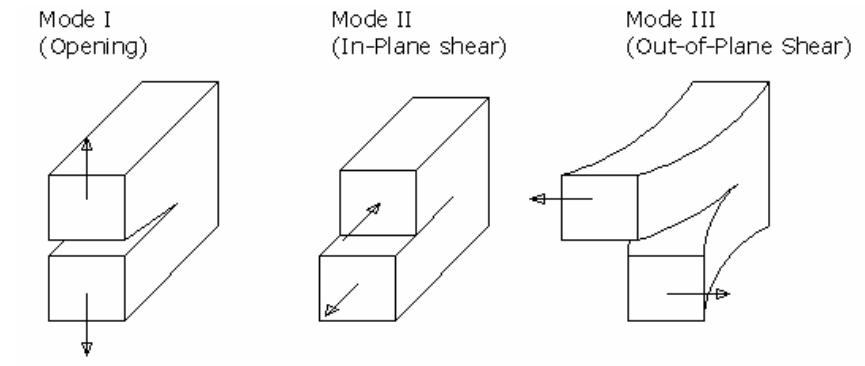


Figure 3.5 The three modes of fracture

In this study the frequently encountered, a fracture mode, the opening mode is selected since the main loading on the flexible rotating disk is the body force. Consequently, due to the position and direction of crack extension, we can name the crack on the fixable rotating disk as a radial crack, a circumferential crack and an arbitrarily oriented crack.

A flexible rotating disk without crack will have a constant stiffness and thus a constant displacement under the body force due to its high angular rotation. However, when the fixable rotating disk contains a crack, the cracked portion of the cross section is not capable of supporting the body force. Thus, a crack behavior called "breathing" will occur, where the displacement as function of the stiffness will be minimum when the crack is closed and maximum when the crack is open. This results in a time dependant stiffness coefficients in the governing equation of the system, and requires making broad simplifying assumption or some type of numerical approximation.

This study focuses on an opening crack which is a through-thickness crack model due to its mostly practical in terms of implementation for a real crack detection and good approximation for the breathing crack. [12, 24, 25].

### 3.3.2 The Strain Energy due to Crack

As it discussed in potential of a rotating disk on page 16, the inertia load is considered as an external load on the system which develop an elastic potential energy i.e. strain energy in the system. Thus, to determine the potential energy due to the crack formation we can use the energy release rate relations.

For linear material, energy release rate $G$ is expressed by, as proposed by Galerkin's proposal,[ 25].

$$G = -\frac{d\pi}{dA_C} \tag{3.29}$$

Where $G$ - energy release rate, $\pi$ - is Potential energy and $A_C$ - is cracked surface area.

And for nonlinear elastic material the energy release rate which relate the potential energy and crack area by the J integral, [ 25 ].

$$J = -\frac{d\pi}{dA_c} \tag{3.30}$$

where $J$ - energy release rate, Besides, for linear elastic material J integral can be considered to be equal to $G$, which be

$$J = G = -\frac{d\pi}{dA_C} \tag{3.31}$$

**3.3.3 J-Contour Integral**

A general formula of the J integral for a crack in an arbitrary body as described by figure 3.6 can be expressed by , while a crack extension along the $\xi$ direction,

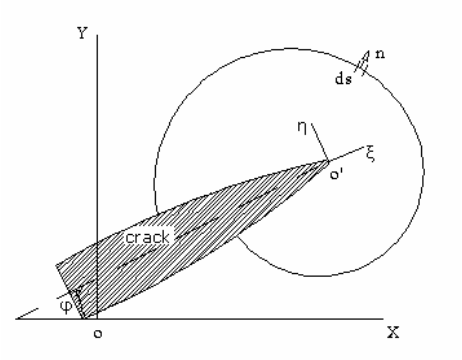


Figure 3.6 An arbitrary contour for a J integral

where X-Y is the global coordinate system and $\xi - \eta$ is local coordinate at crack tip.
a mathematical expression as

$$J = \int_{\Gamma} U_o d\eta - T_i \frac{\partial u_i}{\partial \xi} ds \tag{3.32}$$

Where $U_o = \sigma_{ij} d\varepsilon_{ij}$ is the strain energy density,

$T_i = \sigma_{ij} n_j$ is the traction vector,

$\Gamma$ is an arbitrary contour around the tip of the crack,

$n$ is the unit vector normal to $\Gamma$

$\sigma$, $\varepsilon$, and $u$ are the stress, strain, and displacement fields, respectively

Using an axisymmetric property for the description of local axis $(\varepsilon, \eta)$ at the crack tip the same as that of the local coordinate axis of the rotating disk $(r, \theta)$, Mode I of a radial crack as it seen in figure 5.3 , its J integral expression as given equation (3.32), where $ds = drd\theta$, is obtained to be

$$J = \int_{\Gamma} U_o d\theta - (\sigma_{rr} \frac{\partial u_r}{\partial r} + \sigma_{\theta\theta} \frac{\partial v_\theta}{\partial \theta} + \sigma_{r\theta} \frac{\partial u_r}{\partial r}) drd\theta \qquad (3.33)$$

And for Mode I of a circumferential crack, figure 5.2 is

$$J = \int_{\Gamma} U_o dr - (\sigma_{rr} \frac{\partial u_r}{\partial r} + \sigma_{\theta\theta} \frac{\partial v_\theta}{\partial \theta} + \sigma_{r\theta} \frac{\partial u_\theta}{\partial \theta}) drd\theta \qquad (3.34)$$

where $\sigma_{rr}, \sigma_{\theta\theta}$ and $\sigma_{r\theta}$- are radial, tangential and Shear stresses at a point at radius r and angle $\theta$.

Taking equation (3.33) which express the J integral for a radial crack, the loss of potential energy due to crack formation on the flexible rotating disk can be obtained by substituting equation (3.33) in equation (3.31), thus it yields

$$-\frac{d\pi}{dA_c} = \int_{\Gamma} U_o d\theta - (\sigma_{rr} \frac{\partial u_r}{\partial r} + \sigma_{\theta\theta} \frac{\partial v_\theta}{\partial \theta} + \sigma_{r\theta} \frac{\partial u_r}{\partial r}) drd\theta \qquad (3.35)$$

Following a cross product and an integral procedure, above equation will be

$$\pi = U_C = -\int_{A_C} \left( \int_{\Gamma} U_o d\theta - \left( \sigma_{rr} \frac{\partial u_r}{\partial r} + \sigma_{\theta\theta} \frac{\partial v_\theta}{\partial \theta} + \sigma_{r\theta} \frac{\partial u_r}{\partial r} \right) drd\theta \right) dA_C \qquad 3.36)$$

$$U_C = -\int_{A_C} \left( \int_{\Gamma} U_o d\theta \right) dA_C + \int_{A_C} \left( \int_{\Gamma} \left( \sigma_{rr} \frac{\partial u_r}{\partial r} + \sigma_{\theta\theta} \frac{\partial v_\theta}{\partial \theta} + \sigma_{r\theta} \frac{\partial u_r}{\partial r} \right) drd\theta \right) dA_C \qquad (3.37)$$

Finally using Hamilton's principle for the rotating disk with a through-thickness radial crack can be described as

$$\int_{t_1}^{t_2}(\delta T-\delta U_T)dt=\int_{t_1}^{t_2}(\delta T-\delta(U-U_C)dt=\int_{t_1}^{t_2}(\delta T-\delta U+\delta U_C)dt=0 \tag{3.38}$$

$$\delta\int_{t_2}^{t_2}\left\{\left(\frac{1}{2}V^o\bullet V^o\right)-\left(\frac{1}{2}\int_V\sigma_{ij}\varepsilon_{ij}\right)dV+(U_C)\right\}=0 \tag{3.39}$$

Since the variation for the first two expressions in equation (3.38) has been discussed, let's analyze the term due to the released potential energy due to crack independently

$$\delta\int_{t_1}^{t_2}U_C dt=\delta\int_{t_1}^{t_2}\left\{-\int_{A_C}\left(\int_\Gamma U_o d\theta\right)dA_C+\int_{A_C}\left(\int_\Gamma\left(\sigma_{rr}\frac{\partial u_r}{\partial r}+\sigma_{\theta\theta}\frac{\partial v_\theta}{\partial\theta}+\sigma_{r\theta}\frac{\partial u_r}{\partial r}\right)drd\theta\right)dA_C\right\}dt$$

$$=\delta\int_{t_1}^{t_2}\left\{\left[-\int_{A_C}\left(\int_\Gamma U_o d\theta\right)dA_C\right]+\left[\int_{A_C}\left(\int_\Gamma\left(\sigma_{rr}\frac{\partial u_r}{\partial r}+\sigma_{\theta\theta}\frac{\partial v_\theta}{\partial\theta}+\sigma_{r\theta}\frac{\partial u_r}{\partial r}\right)drd\theta\right)dA_C\right]\right\}dt$$

$$\delta\int_{t_1}^{t_2}U_C dt=\delta\int_{t_1}^{t_2}\left\{\left[-\int_\Gamma\left(\int_{A_C}U_o dA_C\right)d\theta\right]+\right.$$

$$\left.\left[\int_{A_C}\left(\int_\Gamma\left(\sigma_{rr}\frac{\partial u_r}{\partial r}+\sigma_{\theta\theta}\frac{\partial v_\theta}{\partial\theta}+\sigma_{r\theta}\frac{\partial u_r}{\partial r}\right)drd\theta\right)dA_C\right]\right\}dt \tag{3.40}$$

The first integral of equation (3.40) composes the sum of strain energy density on crack surface of the rotating disk. Besides, when this strain energy loss compared with that of total strain energy gain by the flexible rotating disk due to inertia load is very small. Thus we can apply the variation integral only on the second part of equation (3.40) integral, which it will be

$$\delta\int_{t_2}^{t_1}U_C dt=\delta\int_{t_1}^{t_2}\int_{A_C}\left(\int_\Gamma\left(\sigma_{rr}\frac{\partial u_r}{\partial r}+\sigma_{\theta\theta}\frac{\partial v_\theta}{\partial\theta}+\sigma_{r\theta}\frac{\partial u_r}{\partial r}\right)drd\theta\right)dA_C dt \tag{3.41}$$

Since $dA=rdrd\theta$ which is equivalent to $dA/r=drd\theta$, we can express equation (3.41) as

$$\delta\int_{t_2}^{t_1} U_C\,dt = \int_{t_2}^{t_1}\int_{A_C}\left(\int_A \delta\left(\sigma_{rr}\frac{\partial u_r}{\partial r}+\sigma_{\theta\theta}\frac{\partial v_\theta}{\partial\theta}+\sigma_{r\theta}\frac{\partial u_r}{\partial r}\right)\frac{dA}{r}\right)dA_C\,dt \tag{3.42}$$

$$\delta\int_{t_2}^{t_1} U_C\,dt = \int_{t_2}^{t_1}\int_{A}\left(\int_{A_C}\left(\frac{\sigma_{rr}}{r}\frac{\partial}{\partial r}(\delta u)+\frac{\sigma_{\theta\theta}}{r}\frac{\partial}{\partial\theta}(\delta v)+\frac{\sigma_{r\theta}}{r}\frac{\partial}{\partial r}(\delta u)\right)dA_C\right)dA dt$$

$$\delta\int_{t_2}^{t_1} U_C\,dt = \int_{t_2}^{t_1}\int_{A}\left\{\int_{A_C}\left[\left(\frac{\sigma_{rr}}{r}\frac{\partial}{\partial r}+\frac{\sigma_{r\theta}}{r}\frac{\partial}{\partial r}\right)(\delta u)+\frac{\sigma_{\theta\theta}}{r}\frac{\partial}{\partial\theta}(\delta v)\right]dA_C\right\}dA dt \tag{3.43}$$

where the bracket of equation (4.43) compose components along

- the radial $\frac{A_C}{r}\left(\frac{\partial\sigma_{rr}}{\partial r}+\frac{\partial\sigma_{r\theta}}{\partial r}\right)$ and
- tangential $\frac{A_C}{r}\left(\frac{\partial\sigma_{\theta\theta}}{\partial\theta}\right)$ coordinates direction.

Finally, the equations of motion for the flexible rotating disk with crack can be derived by substituting the radial and tangential components of equation (3.43) in equation (3.22) and (3.23) for the radial and tangential displacements as well equation (3.2) for the stress and force relation, the displacements equations of the flexible rotating disk with crack along the radial, tangential and transverse direction obtained as

$$\rho h\left(\frac{\partial^2 u}{\partial t^2}-2\Omega\frac{\partial v}{\partial t}-\Omega^2 u\right)-\frac{\partial q_r}{\partial r}-\frac{\partial q_{r\theta}}{r\partial\theta}-\frac{q_\theta}{r}=\rho h\Omega^2 r+\frac{1}{r}\frac{A_C}{A}\left(\frac{\partial q_r}{\partial r}+\frac{\partial q_{r\theta}}{\partial r}\right) \tag{3.45}$$

$$\rho h\left(\frac{\partial^2 v}{\partial t^2}+2\Omega\frac{\partial u}{\partial t}-\Omega^2 v\right)-\frac{\partial q_\theta}{r\partial\theta}-\frac{\partial q_{r\theta}}{\partial r}-\frac{q_{r\theta}}{r}=\frac{1}{r}\frac{A_C}{A}\left(\frac{\partial q_{\theta\theta}}{\partial\theta}\right) \tag{3.46}$$

$$\left\{\rho h\left(\frac{\partial^2 w}{\partial t^2}+2\Omega\frac{\partial^2 w}{\partial t\partial\theta}+\Omega^2\frac{\partial^2 w}{\partial\theta^2}\right)+D\nabla^4 w-\frac{\partial}{r\partial r}\left[r\left(q_r\frac{\partial w}{\partial r}+q_{r\theta}\frac{\partial w}{r\partial\theta}\right)\right]\right.$$
$$\left.-\frac{\partial}{r\partial\theta}\left(q_{r\theta}\frac{\partial w}{\partial r}+q_\theta\frac{\partial w}{r\partial\theta}\right)\right\}=0 \tag{3.47}$$

The boundary conditions of the flexible rotating disk without crack are the same as that for the flexible rotating disk with crack as it expressed in equations (3.26) and

(3.27). We call the differential equation (3.45) – (3.47) with boundary conditions (3.26) and (3.27) the **strong form** of the differential equation.

# 4 Finite Element Formulation

## 4.1 Introduction

It is a basic fact that most practical problems in engineering are governed by differential equation. The governing equation of the flexible rotating disk with a through-thickness crack is in partial differential form. Owing to complexities of geometry and some-how the loading, finding exact solutions to those governing equations might not be possible. Thus approximate techniques for solving differential equation are implemented for this study. Indeed, the finite element method is one of such techniques that yields good approximation, [ 26, 27, 28].

As it has been discussed previously, the three dimensional flexible rotating disk has been modeled by circular plate which is exposed to high rotating angular speed. Thus, the plate elements are considered to be subjected to both in plane and transverse displacement.

## 4.2 The Weak Form

One of the step in the finite element formulation is to find the *weak form* from the *strong form*, which is the partial differential form of the governing equation of the flexible rotating disk (3.23), (3.24) and (3.25) and the associated boundary conditions given by equation (3.26) and (3.27). But before this step is conducted, the trial and weighting functions should be defined. The trial functions are function in the [1]Hilbert space $H^1$,[34] which satisfy both the essential and natural boundary conditions,[ 9 ]. Denoting the trial function in the $r, \theta \, and \, z$ directions by $u, v \, and \, w$, they can be defined as:

$$(u,v) \in V_{uv} = \left\{ (u,v) \middle| u \in H^1, v \in H^1, \right.$$

$$\left. u\big|_{r=a} = 0, v\big|_{r=a} = 0, q_r\big|_{r=b} = 0, q_{r\theta}\big|_{r=b} = 0 \right\} \qquad (4.1)$$

[1]A Hilbert space is an abstract vector space in which distances and angles can be measured, which is "complete", meaning that if a sequence of vectors approaches a limit, then that limit is guaranteed to be in the space as well.

$$w \in V_w = \{w | w \in H^1, \partial w/\partial r \in H^1, \partial w/\partial \theta \in H^1, w|_{r=a} = 0, \partial w/\partial r|_{r=a} = 0, m_r|_{r=b} = 0,$$
$$-D\partial\nabla^2 w/\partial r + \partial m_{r\theta}/r\partial\theta|_{r=b} = 0\} \quad (4.2)$$

where $V_{uv}$ and $V_w$ are the trial function space for the radial and tangential and transverse displacement respectively. Note that, equation (4.2) implies that both the transverse displacement and its derivatives should be in Hilbert space as a result of the plate theory which describe the degree of freedom by displacement as well the slopes.

And the weighting function is defined as an arbitrary function, which is zero on the boundary where the essential boundary conditions are prescribed. Therefore, the weighting functions for the radial, tangential and transverse displacement, which are represented by $W_1, W_2 \; and \; W_3$, are given by

$$(W_1, W_2) \in \overline{V}_{uv} = \{(W_1, W_2) | W_1 \in H^1, W_2 \in H^1, W_1|_{r=a} = 0, W_2|_{r=a} = 0\}, \quad (4.3)$$

$$W_3 \in \overline{V}_w = \{W_3 | W_3 \in H^1, \partial W_3/\partial r \in H^1, \partial W_3/\partial\theta \in H^1,$$
$$W_3|_{r=a} = 0, \partial W_3/\partial r|_{r=a} = 0\} \quad (4.4)$$

To obtain the weak form, the first step is to multiply equation (3.23), (3.24) and (3.25) by the weighting function the $W_1, W_2 \; and \; W_3$, respectively, and followed by an integration of this equation over the disk area A.

$$\int_A W_1 \left[ \rho h \left( \frac{\partial^2 u}{\partial t^2} - 2\Omega \frac{\partial v}{\partial t} - \Omega^2 u \right) - \frac{\partial q_r}{\partial r} - \frac{\partial q_{r\theta}}{r\partial\theta} - \frac{q_\theta}{r} - \rho h \Omega^2 r \right.$$
$$\left. - \frac{1}{r}\frac{A_C}{A}\left( \frac{\partial q_r}{\partial r} + \frac{\partial q_{r\theta}}{\partial r} \right) \right] = 0 \quad (4.5)$$

$$\int_A W_2 \left[ \rho h \left( \frac{\partial^2 v}{\partial t^2} + 2\Omega \frac{\partial u}{\partial t} - \Omega^2 v \right) - \frac{\partial q_\theta}{r\partial\theta} - \frac{\partial q_{r\theta}}{\partial r} - \frac{q_{r\theta}}{r} - \frac{1}{r}\frac{A_C}{A}\left( \frac{\partial q_{\theta\theta}}{\partial\theta} \right) \right] = 0 \quad (4.6)$$

$$\int_A W_3 \left\langle \left\{ \rho h \left( \frac{\partial^2 w}{\partial t^2} + 2\Omega \frac{\partial^2 w}{\partial t \partial\theta} + \Omega^2 \frac{\partial^2 w}{\partial\theta^2} \right) + D\nabla^4 w - \frac{\partial}{r\partial r}\left[ r\left( q_r \frac{\partial w}{\partial r} + q_{r\theta} \frac{\partial w}{r\partial\theta} \right) \right] \right.$$

$$-\frac{\partial}{r\partial\theta}\left(q_{r\theta}\frac{\partial w}{\partial r}+q_{\theta}\frac{\partial w}{r\partial\theta}\right)\Bigg\}\Bigg\rangle=0 \qquad (4.7)$$

Before applying the Galerkin's method of approximation on equation (4.5) , (4.6) and (4.7) which can be fully coupled with each other, as a results leads to derive one weak from, the necessary formulation are:

### 4.2.1 The Displacement Formulation

The essential step consisted of approximating the variation of displacement in the element should be done with suitable functions. Thus, an eight node annular element, figure 4.1, is chosen to approximate the variation of displacement within an element in terms of the displacement at the nodes of the element. Where, this model for the displacement formulations are choose taking into consideration, the displacement function is continues with in the element, its capability of representing rigid body displacement of the element, and since the boundary curvature of the flexible rotating disk is curved. By assuming a linear displacement variation inside the element, the displacement model can be modeled as it been seen figure 4.1. Beside a classical interpolation polynomial has been chosen for this study in addition to natural interpolation polynomial because the governing differential equation composed of a higher order, biharmonic $(\nabla^4 w=0)$. Thus, is $C^1$ continuity is required which states a continuity in addition to $u$ *and* $v$, consideration for continuity along $\frac{\partial w}{\partial n}$ in inside and between elements should be encountered.

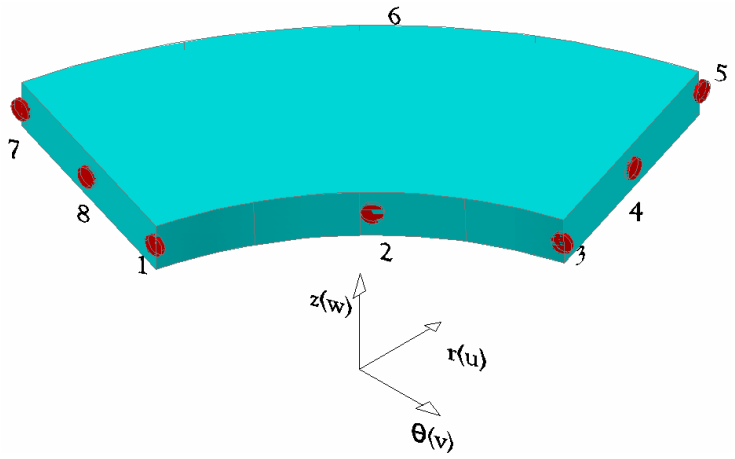


Figure 4.1 An eight node element with its degree of freedom

Thus the degree of freedom at each node will be $u, v, w, \frac{\partial w}{\partial r}, \frac{\partial w}{\partial \theta}, \frac{\partial^2 w}{\partial r \partial \theta}$. Using the natural interpolation polynomial methods, the displacement model along radial and tangential direction is set as

$$\vec{U} = \begin{Bmatrix} u(r,\theta) \\ v(r,\theta) \end{Bmatrix} = [N(r,\theta)]_A^T \begin{Bmatrix} u \\ v \end{Bmatrix} \tag{4.8}$$

Where

$$[N(r,\theta)]_A = \begin{bmatrix} N_1 & 0 & - & - & - & 0 & N_8 & 0 \\ 0 & N_1 & 0 & - & - & - & 0 & N_8 \end{bmatrix}_{2\times 16} \tag{4.9}$$

And using a conforming element made by Bogner-Fox-Schmit (BFS-16), the displacement model along the transverse is set as:

$$\vec{W} = w(r,\theta) = [N(r,\theta)]_B^T \begin{Bmatrix} w \\ \frac{\partial w}{\partial r} \\ \frac{\partial w}{\partial \theta} \\ \frac{\partial^2 w}{\partial r \partial \theta} \end{Bmatrix} \tag{4.10}$$

Where,

$$[N(r,\theta)]_B = \left[H_{0i}^{(1)}(r)H_{0j}^{(1)}, H_{1i}^{(1)}(r)H_{0j}^{(1)}(\theta), H_{0i}^{(1)}(r)H_{1j}^{(1)}(\theta), H_{1i}^{(1)}(r)H_{1j}^{(1)}(\theta)\right]^T \tag{4.11}$$

For i and j =1, 2 the shape function is defined by Hermitian polynomial. While the first order Hermite polynomial can be defined as

$$H_{01}^{(1)}(r) = \frac{1}{l^3}(2r^3 - 3lr^2 + l^3) \qquad H_{01}^{(1)}(\theta) = \frac{1}{l^3}(2\theta^3 - 3l\theta^2 + l^3)$$

$$H_{02}^{(1)}(r) = -\frac{1}{l^3}(2r^3 - 3lr^2) \qquad H_{02}^{(1)}(\theta) = -\frac{1}{l^3}(2\theta^3 - 3l\theta^2)$$

and

$$H_{11}^{(1)}(r) = \frac{1}{l^2}(r^3 - 2lr^2 + l^2 r) \qquad H_{11}^{(1)}(\theta) = \frac{1}{l^2}(\theta^3 - 2l\theta^2 + l^2\theta)$$

$$H_{12}^{(1)}(r) = \frac{1}{l^2}(r^3 - lr^2) \qquad H_{12}^{(1)}(\theta) = \frac{1}{l^2}(\theta^3 - l\theta^2)$$

Where $l$ is the element length.

The combined element displacements vector at nodal point will be

$$d^e = \left\{ u_1, v_1, w_1, \left(\frac{\partial w}{\partial r}\right)_1, \left(\frac{\partial w}{\partial \theta}\right)_1, \left(\frac{\partial^2 w}{\partial r \partial \theta}\right)_1 + u_2, v_2, w_2, \left(\frac{\partial w}{\partial r}\right)_2, \left(\frac{\partial w}{\partial \theta}\right)_2, \left(\frac{\partial^2 w}{\partial r \partial \theta}\right)_2 + \ldots \right.$$

$$\left. \ldots + u_8, v_8, w_8, \left(\frac{\partial w}{\partial r}\right)_8, \left(\frac{\partial w}{\partial \theta}\right)_8, \left(\frac{\partial^2 w}{\partial r \partial \theta}\right)_8 \right\}^e \tag{4.12}$$

### 4.2.2 The Kinematics Equations

Taking into consideration the displacement of plate element due to membrane and bending effect, the relationship between strains to displacements can be expressed as:

$$\left\{\varepsilon^L\right\} = \begin{Bmatrix} \varepsilon^m \\ \varepsilon^b \end{Bmatrix} = \begin{Bmatrix} [\varepsilon_r, \varepsilon_\theta, \varepsilon_{r\theta}]^T \\ [k_r, k_\theta, k_{r\theta}]^T \end{Bmatrix} = \begin{Bmatrix} \left[\frac{\partial u}{\partial r}, \frac{\partial v}{r\partial \theta} + \frac{u}{r}, \frac{1}{2}\left(\frac{\partial u}{\partial r} + \frac{\partial v}{\partial r} - \frac{v}{r}\right)\right]^T \\ \left[\frac{\partial^2 w}{\partial r^2}, -\left(\frac{\partial w}{r\partial r} + \frac{\partial^2 w}{r^2 \partial \theta^2}\right), -2\left(\frac{\partial^2 w}{r\partial r \partial \theta} - \frac{\partial w}{r^2 \partial \theta}\right)\right]^T \end{Bmatrix} \tag{4.13}$$

Thus the component of the strain can be expressed in terms of nodal displacement as

$$\{\varepsilon\} = [B]\{d^e\} \tag{4.14}$$

Where

$$[B] = \begin{bmatrix} \frac{\partial N_i}{\partial r} & 0 & 0 & 0 & 0 & 0 \\ \frac{N_i}{r} & \frac{\partial N_i}{r\partial \theta} & 0 & 0 & 0 & 0 \\ \frac{\partial N_i}{r\partial \theta} & \left(\frac{\partial N_i}{\partial r} - \frac{N_i}{r}\right) & 0 & 0 & 0 & 0 \\ 0 & 0 & 0 & -\frac{\partial N_i}{\partial r} & 0 & 0 \\ 0 & 0 & 0 & \frac{N_i}{r} & \frac{\partial N_i}{r\partial \theta} & 0 \\ 0 & 0 & 0 & 0 & \frac{N_i}{r^2} & -\frac{N_i}{r} \end{bmatrix} \tag{4.15}$$

Taking in to consideration for those relation that been formulated, summing equations (4.5) , (4.6) and (4.7) which then the weak form (integrate form) of resultant equation over the disk area A became

$$\rho h\int_A \overline{W}^T \frac{\partial^2 \mathbf{u}}{\partial t^2} dA + 2\Omega\rho h\int_A \overline{W}^T \Phi_g \frac{\partial \mathbf{u}}{\partial t} dA - \Omega^2 \rho h\int_A \overline{W}^T \Phi_k \mathbf{u} dA$$
$$+\int_A (\overline{\varepsilon}^L)^T D\varepsilon^L dA + \frac{1}{r}\frac{A_C}{A}\int_A (\overline{\varepsilon_P^L})^T D\varepsilon_P^L dA + \int_A \overline{\theta}^T Q\theta dA = \int_A \overline{W}^T F dA \qquad (4.16)$$

Where $\mathbf{u} = \begin{Bmatrix} u \\ v \\ w \end{Bmatrix}$ $\overline{W} = \begin{Bmatrix} W_1 \\ W_2 \\ W_3 \end{Bmatrix}$ $\theta = \begin{Bmatrix} \frac{\partial w}{\partial r} \\ \frac{\partial w}{r\partial\theta} \end{Bmatrix}$ $\overline{\theta} = \begin{Bmatrix} \frac{\partial W_3}{\partial r} \\ \frac{\partial W_3}{r\partial\theta} \end{Bmatrix}$

$$\Phi_k = \begin{bmatrix} 1 & 0 & 0 \\ 0 & 1 & 0 \\ 0 & 0 & -\frac{\partial^2 w}{\partial\theta^2} \end{bmatrix} \qquad F = \begin{bmatrix} \rho h\Omega^2 r \\ 0 \\ 0 \end{bmatrix} \qquad Q = \begin{bmatrix} q_r & q_{r\theta} \\ q_{r\theta} & q_\theta \end{bmatrix}$$

$$\overline{\varepsilon}^L = \left\{ \frac{\partial W_1}{\partial r}, \frac{\partial W_2}{r\partial\theta} + \frac{W_1}{r}, \frac{\partial W_1}{r\partial\theta} + \frac{\partial W_2}{\partial r} - \frac{W_2}{r}, \right.$$
$$\left. -\frac{\partial^2 W_3}{\partial r^2}, -\frac{1}{r}\left(\frac{\partial W_3}{\partial r} + \frac{\partial^2 W_3}{r\partial\theta^2}\right), -\frac{2}{r}\left(\frac{\partial^2 W_3}{\partial r\partial\theta} - \frac{\partial W_3}{r\partial\theta}\right) \right\}^T \qquad (4.17)$$

A different shape function as in equation 4.11 for elements around the crack tip is used from those elements enclosed in the flexible rotating disk for advantage of following the singularity effect at those regions. That is because, in linear elastic problem, it has been shown that the displacement near the crack tip vary as $\sqrt{r}$ , where r is the distance from the crack tip. And the stress and strains are singular at the crack tip, varying as $1/\sqrt{r}$ . Thus to pick up the singularity in strain, the crack face should be coincident and the element around the crack tip should be quadratic, with the midside nodes placed at the quarter points. The singular element which is selected for this study is shown in figure 4.6.

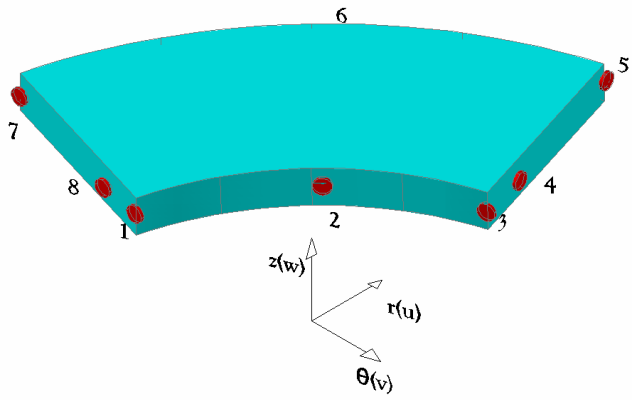


Figure 4.2 Eight node annular element at crack tip regions

The trial function vector for $u$ can be defined as

$$u = N^T d^e, \tag{4.18}$$

Where the shapes function $N$ that is a function of $r$ *and* $\theta$ assigned as:

$$N(r,\theta) = \begin{bmatrix} N_{Aii} & 0 & 0 \\ 0 & N_{Aii} & 0 \\ 0 & 0 & N_{Bij} \\ N_{Bij} & 0 & 0 \\ 0 & N_{Bij} & 0 \\ 0 & 0 & N_{Bij} \end{bmatrix}_{48*3} \quad \text{Where i,j=1,2,...,8} \tag{4.19}$$

Similarly for $\theta$ vector in equation (4.16) can be written as

$$\theta = N_\theta^T d^e \tag{4.20}$$

Where the shapes function $N_\theta$ that is function of $r$ *and* $\theta$ assigned

$$N_\theta(r,\theta) = \begin{bmatrix} 0 & 0 & 0 \\ 0 & 0 & 0 \\ 0 & 0 & 0 \\ N_{Bij} & 0 & 0 \\ 0 & N_{Bij}/r & 0 \\ 0 & 0 & 0 \end{bmatrix}_{48*3} \quad \text{Where i,j=1,2,...,8} \tag{4.21}$$

Further, the weighting function vectors $\overline{W}, \overline{\theta}$ are given by

$$\overline{W} = N^T \overline{d}^e \tag{4.22}$$

$$\overline{\theta} = N_\theta^T \overline{d}^e \tag{4.23}$$

And for the weighting function of $\overline{\varepsilon}^L$ it can be expressed by using equation (4.14) as

$$\overline{\varepsilon}^L = B\overline{d}^e \tag{4.24}$$

Where $\overline{d}^e$ is an arbitrary $48\times1$vector.

**4.3 Spatial Discretization**

The flexible rotating disk is modeled with a through-thickness crack and the discretization for the area is done using eight node annular elements. The process of discretization is essentially depending on the exercise of the analyst judgment. For this study, a discretization process that minimized errors and guarantees good range of accuracy is implemented. To achieve this accuracy, as it been discussed earlier, an eight-node annular element is selected for its advantage of modeling curved boundaries of the flexible rotating disk model and for yielding good solution with minimum element number. More over, this quadratic element model has an advantage in that it can modeled to be designed so that the cracks tip singularity effect can to be incorporated easily.

Thus, let the disk is discretized by $N_e$ i.e finite N elements, which had a trial function as described above. Then substitution of strain-deformation relation equation (4.14) and trial functions equation (4.18), (4.20), (4.22)-(4.24) in to the integral form of the governing equation of the rotating disk equation (4.16). And applying finite element formulation techniques, thus the result became as:

$$\sum_{e=1}^{N_e}\left(\overline{d}^e\right)^T\left\{m^e\ddot{d}^e + 2\Omega g^e\dot{d}^e + [K^e - SK_c^e]d^e + P^e\right\} = \sum_{e=1}^{N_e}\left(\overline{d}^e\right)^T F^e \tag{4.25}$$

Where, for element area of $A_e$

$$m^e = \rho h \int_{A_e} NN^T dA, \quad g^e = \rho h \int_{A_e} N \Phi_g N^T dA, \quad K^e = \int_{A_e} B^T DB dA,$$

$$K_c^e = \int_{A_e} B_p^T DB_p dA, \ {}^*S = 1/r(A_c/A), \ P^e = \left( \int_{A_e} N_\theta Q N_\theta^T dA \right) d^e, \ F^e = \int_{A_e} NF dA \quad (4.26)$$

Note that, all matrixes in equation (4.26) are $48 \times 48$ matrix while the element internal force vector $P^e$ and the element load vector $F^e$ are $48 \times 1$ vectors. And, $K_c$ is the stiffness coefficient due to crack.

### 4.4 Assembly to Global Matrix Form

An arbitrary vector, $\overline{d}^e$, for which the set of the ordinary differential equations that can be obtained in matrix vector form during the assembly procedure. Thus the global matrix vector is obtained by assembling the element matrix and their vectors of equation (4.25). The global equation result as:

$$\mathbf{M}\ddot{\mathbf{d}} + 2\Omega\mathbf{G}\dot{\mathbf{d}} + [\mathbf{k} - S\mathbf{k_c}]\mathbf{d} + \mathbf{P(d)} = \mathbf{F} \quad (4.27)$$

Where

- $\mathbf{M}$ is the global mass matrix, which expressed by

$$\mathbf{M} = \underset{e=1}{\overset{N_e}{A}} m^e, \quad (4.28)$$

- $\mathbf{d}$ is the global displacement vector ,which expressed by

$$\mathbf{d} = \left\{ u_1, v_1, w_1, \left(\frac{\partial w}{\partial r}\right)_1, \left(\frac{\partial w}{\partial \theta}\right)_1, \left(\frac{\partial^2 w}{\partial r \partial \theta}\right)_1, \ldots\ldots, +u_{N_e+1}, v_{N_e+1}, w_{N_e+1}, \right.$$

$$\left. \left(\frac{\partial w}{\partial r}\right)_{N_e+1}, \left(\frac{\partial w}{\partial \theta}\right)_{N_e+1}, \left(\frac{\partial^2 w}{\partial r \partial \theta}\right)_{N_e+1} \right\}^T \quad (4.29)$$

- $\mathbf{k}$ is the global stiffness matrix, which expressed by

$$\mathbf{k} = \underset{e=1}{\overset{N_e}{A}} k^e, \quad (4.30)$$

*S constant coefficient for crack stiffness in terms of the crack type and its configuration

- $\mathbf{k_c}$ is the localized stiffness matrix due to crack( i.e. in the region of crack), expressed by

$$\mathbf{k_c} = \underset{e=1}{\overset{N_e}{A}} k_c^{\,e}, \tag{4.31}$$

- The non-linear global internal force vector $\mathbf{P(d)}$ and the global load vector $\mathbf{F}$ can be expressed as

$$\mathbf{P(d)} = \underset{e=1}{\overset{N_e}{A}} P^e, \qquad \mathbf{F} = \underset{e=1}{\overset{N_e}{A}} F^e, \tag{4.32}$$

Where "$A$" denotes the assembly operator.

Noting that the governing equation of the flexible rotating disk (4.27) with crack is a non-liner equation of motion because $\mathbf{P}$ is a function of $\mathbf{d}$. Hence, to obtain the natural frequency and mode shape of the flexible rotating disk, equation (4.27) should be linearized. Thus, a perturbation method of linearization the non-linear equation is applied,[23,31,36].

For dynamic steady state condition, i.e. $\dot{\Omega}$=0 because of constant angular rotation, the displacement vector can be written as

$$d = d^* + \Delta d \tag{4.33}$$

Where: $d^*$ =the displacement vector of the equilibrium position

$\Delta d$ =perturbation displacement vector from equilibrium position

Substituting equation (4.33) into equation (4.27) yields the dynamic equilibrium equation in a steady state and a perturbed equation from the equilibrium position. The equilibrium equation is given by

$$[K - SK_c]d^* + P(d^*) = F \tag{4.34}$$

And since equation (4.37) is non-linear, the equilibrium position vector d* can be obtained by a non-linear equation solver. The perturbed equation is

$$M\Delta\ddot{d} + 2\Omega G\Delta\dot{d} + [K - SK_c + K_T]\Delta d = 0 \tag{4.35}$$

Where is the tangent matrix at the equilibrium position, defined by

$$K_T = \left.\frac{\partial P}{\partial d}\right|_{d=d^*} \tag{4.36}$$

Finally, the linear governing equation of rotating disk with crack in matrix form is expressed by equation (4.35).

# Chapter Five

## 5 Solution Techniques

### 5.1 Introduction

The governing equations of the rotating disk without and with crack are developed in chapter four, see equation (3.45), (3.46) and (3.47). And in chapter five the governing equation is expressed by matrix form equation (4.38). In this chapter, solution options taking into consideration the objectives of thesis are applied to find solution for those governing equations.

ANSYS, which is a complete finite element analysis (FEA) simulation software package developed by **ANSYS** Inc-USA, is used to simulate the essential condition, inertia load and boundary conditions, restrained effect of the system at middle bore. Further, it helps to determine the geometric modeled response to specified condition. The geometric models, which simulate the physical components (rotating disk without and with crack) are used as an input for finite element analysis in ANSYS software.

However, ANSYS software is capable of modeling physical components in geometric models finite element analysis, another commercial software **SolidWorks** used for geometric modeling in this study. SolidWorks employs a parametric, feature-based approach for creating models and assemblies. The reason behind for selecting this software for geometric modeling is due to the complicated features of the physical components such as different profile of notches for modeling crack, gear teeth to imitate blade on the rotating disk and the disk cross-section.

The procedures followed for determining solution for selected solution options discussed below.

### 5.2 Geometric Modeling

The geometric models that simulate the physical components of rotating disk without and with crack for analysis purpose are discussed below. Models that have been done taking in to account the objective of the thesis are

i. Rotating Disk without crack: The designed geometric model of the rotating disk without crack had an outside diameter of 9.25 in. and a bore thickness and outside rim thickness of 1.00 in. and 1.25 in., respectively. The thinnest portion of the web is 0.10 in., with the cross-section and height dimensions of the blades being 1.25 in. × 0.13 in. and 0.33 in., respectively. Lastly, eight holes, 0.20 in. diameter each, were placed midway in the rim section. The eight holes were evenly spaced. The holes are to be utilized for possible mass attachments or used for future notch initiation points. The geometric model is seen figure 5.1.

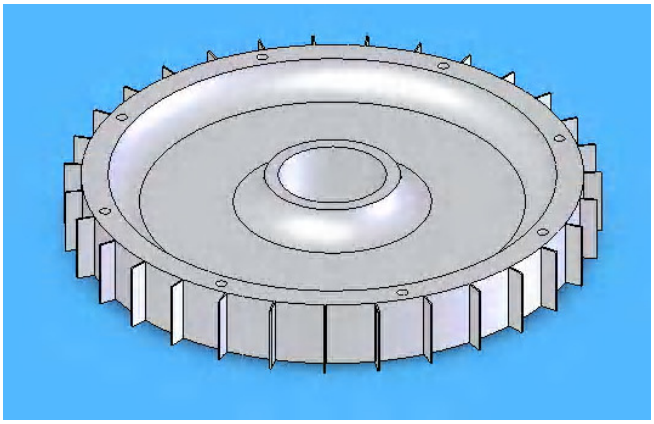

Figure 5.1 rotating disk without crack

ii. Rotating Disks with circumferential crack: This geometric models are designed with the same dimension of the rotating disk without crack geometric values except that on this model, circumferentially oriented notches is added at radius R=2.12in to simulate circumferential crack. Figure 5.2 shows a rotating disk with circumferential notch subtending an angle of $6^0$.

For better understanding the behavioral change that might rise due subtend angle for circumferential crack, different angle values have been used in the analysis. Selected subtended angle $\theta$ are $12^0$,$18^0$,$24^0$,$26^0$,$32^0$ , which in parallel used as an input parameter for analysis of the rotating disk with-out and with crack.

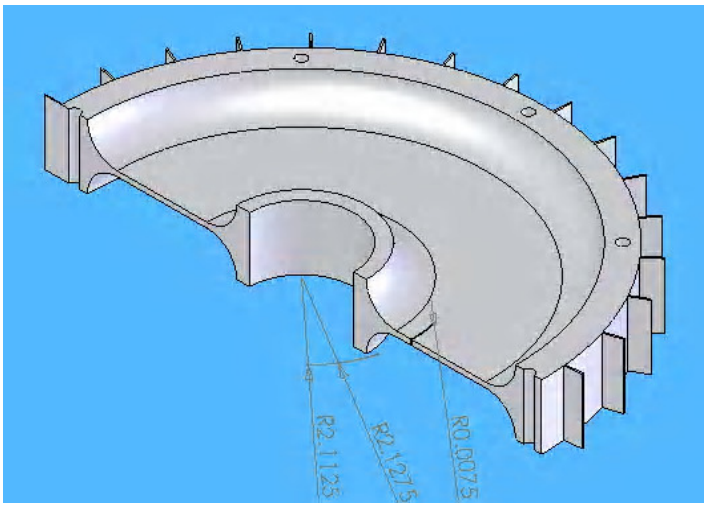


Figure 5.2 Rotating Disk with circumferential notch sustained angle of $28^0$

iii. Rotating Disks with radial crack: The same procedures are followed for modeling rotating disks with radial crack as for modeling Rotating Disks with circumferential crack. Besides, notch orientations in these models are along radial direction. For investigation of change in length of crack with behavioral change in models different notch lengths are used for analysis. These are 0.222in, 0.444in and 0.666in. Figure 5.3 shows one of the rotating disks with radial notch of 0.444in in length.

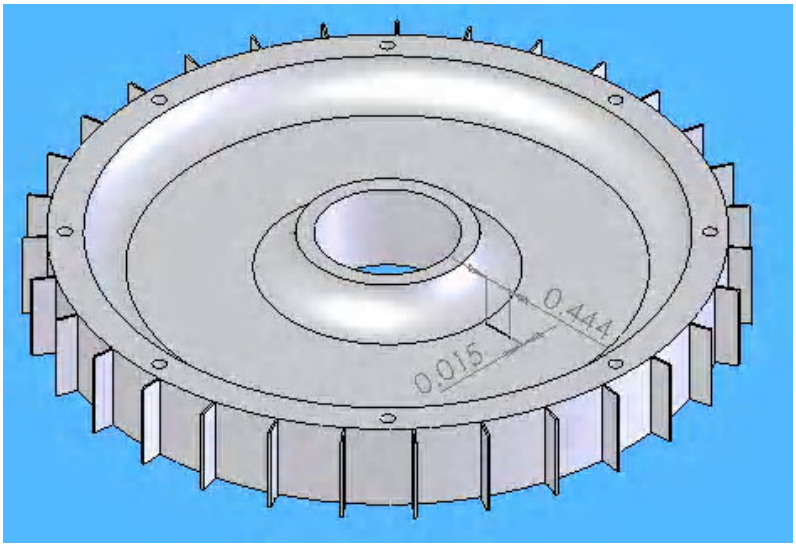


Figure 5.3 Rotating Disk with radial notch at radial center $R_C$=2.12in

iv. Rotating Disks with an arbitrarily oriented crack: These geometric models are designed following the same procedure as rotating disk without crack model. In advance, these models are designed with a notch at different angle of β from radial axis. These models are expected to describe the behavior and physical change of a model with the change of crack orientation from radial axis to tangential axis. For notch length of 0.444in, Selected angle β are $15^0$, $30^0$,$45^0$,$60^0$,$75^0$ from radial axis.

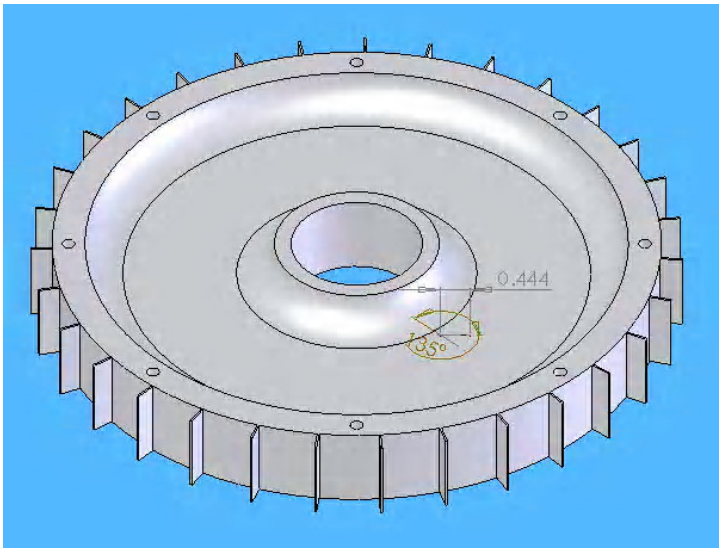


Figure 5.4 Rotating Disk with arbitrary notch at radial center $R_C$=2.12in
[Notch length L=0.444in at 45° from radial axis]

Note: Modeled notches are assigned on position where the Rotating Disk without crack is highly stressed region owing to the centrifugal load i.e. radial center R=2.12in. Moreover, modeled notch dimensions are adapted from one of the research carried by NASA research center, [4]. Thus, the width of the notch is done by imitate the dimensions of a wire thickness equal to 0.12in and the height of the crack is specified to be equal to the web section thickness of the models.

All geometric models, modeled by **SolidWorks** had been imported to the finite element analsysis software, **ANSYS**, for analysis purpose.

## 5.3 Discritizing the Model

The discritizing element used for analysis, which their sum of response in the model rise to the total response of the complete geometric model is specified from ANSYS element library. A solid model element, 20 solid 95, which satisfy the characteristic need in discritzing the geometric model as per the objectives of the analysis criteria is selected.

## 5.4 Material Selection

Most commonly used material for production of Rotating Disk, nickel alloy (i.e. Haynes X-750) is selected as material input for the analysis. The material properties for Haynes X-750 are Young Module's $E=31\times10^3$ Kpsi, Poison's ratio $\upsilon=0.3$ and Density $\rho=0.31 lb/in^3$. Perhaps, design limitation to burst failure due angular rotation for a model with this material equal 25000rpm.

## 5.5 Finite Element Modeling( Mesh Generation)

In this step, previously defined geometric models in ANSYS software is further defined by meshed finite elements and nodes. Thus, the geometric model with finite element will simulate the physical components in more suitable form as well it will be more preferable to obtain approximate results to the exact result of the solution from the analysis.

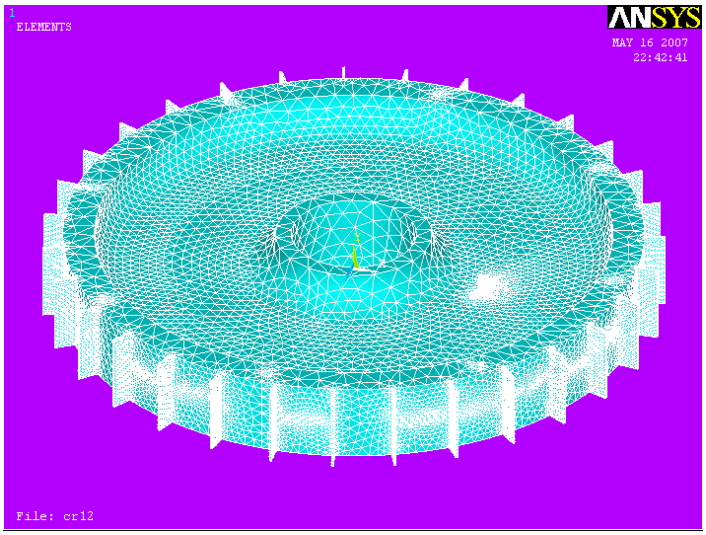


Figure 5.5 Discritization of geometric model with finite elements

Density of the generated meshes is controlled at global and at local level. A default option “smart sizing” for specifying element sizes at global level is applied. And for the benefit of keeping singularities at crack tip “keypoint sizing” for concentrating the middle nodes of element around crack tip are specified to shift to corner nodes,[ 1].

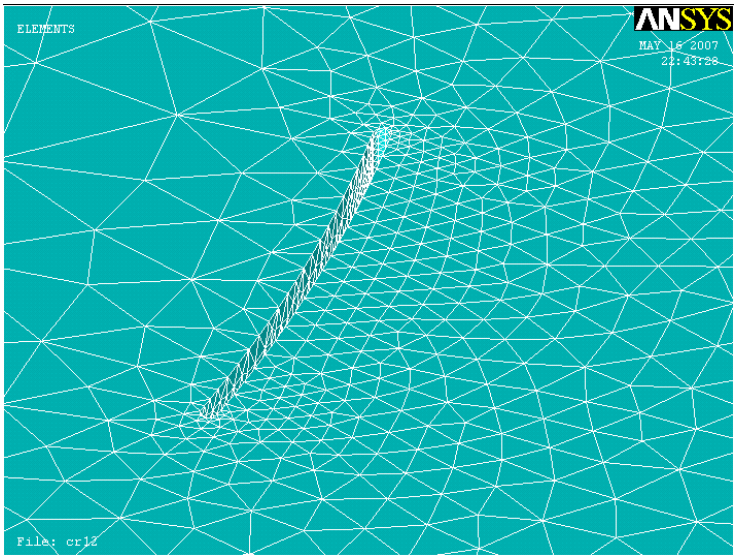

Figure 5.6 Distribution of elements at crack surface

## 5.6 Apply Loads

In this step, essential and boundary conditions are specified. Where, one of the loading conditions for the analysis is to constraint, the inner surface of the middles bore of the geometric model from translational motion along x, y and z axis and a rotational motion along x and z axis. This step helps to define the boundary condition for satisfying the physical system joint (i.e. to restrain the rigid body) between rotating disk and shaft.

In addition, an essential condition for the benefit of encountering the inertia effect is specified i.e. in terms of angular velocity along y-axis. Specified angular velocity values with in the design angular velocity limit of the model are 2000rpm, 4000rpm, 6000rpm, 8000rpm and 10000rpm, which are taking as an advantage for there can be used as input parameters for analysis.

### 5.7 Defined Analysis Solution Options

At this step, Analysis types are selected in terms of expected result that could characterize the components from either the components exposed to damage (cracked) or not. Among from few analysis options provided in the finite element analysis software ANSYS, a modal and static analysis are carried out taking into consideration the objective of this thesis. The modal analysis are carried out for investigation of the change in disk rotating disks vibration characteristic such as natural frequency and mode shapes. And, static analysis is carried out for determining the distribution of deformation and stresses on the rotating disks due to inertia load.

## 6 Result and Discussion

In chapter five, steps and input parameters that are used in the analysis of the rotating disk without and with crack discussed briefly. In this chapter, results from the analysis in relation to input parameters will be discussed. To remind ourselves what input parameters are used for analysis, they are different angular speeds, different crack orientation, different crack length and a range for crack sustained angle. They are specified to investigate the behavioral change of the rotating disk when it is exposed to crack.

It should be noted that in this thesis only the disk mounted on the shaft is considered and the effect of blades mounted on the edge of the disk is not considered in the analysis. Thus, only the inertia effect of the rotating disk is considered by its angular rotation.

Taking into account that understanding the behavior of the rotating disk without crack is important for comparison, its analysis is carried first. Table 6.1 presents the first ten natural frequencies of the rotating disk without crack that obtained from the modal analysis of the finite element model using ANSYS.

Table 6.1: Natural frequency Rotating Disk without crack

| Expanded modes | Natural frequency(Hz) |
|---|---|
| 1 | 19.01953789191 |
| 2 | 19.27573053682 |
| 3 | 28.61926001242 |
| 4 | 63.15635104316 |
| 5 | 63.16425780515 |
| 6 | 84.72076098343 |
| 7 | 175.7252920167 |
| 8 | 175.7732168761 |

| Expanded modes | Natural frequency(Hz) |
|---|---|
| 9 | 205.7563083334 |
| 10 | 205.7766322548 |

And, the first four mode shapes corresponding to the first four natural frequencies of the rotating disk without crack are illustrated in figure 6.1 ( a ) - ( d ) .

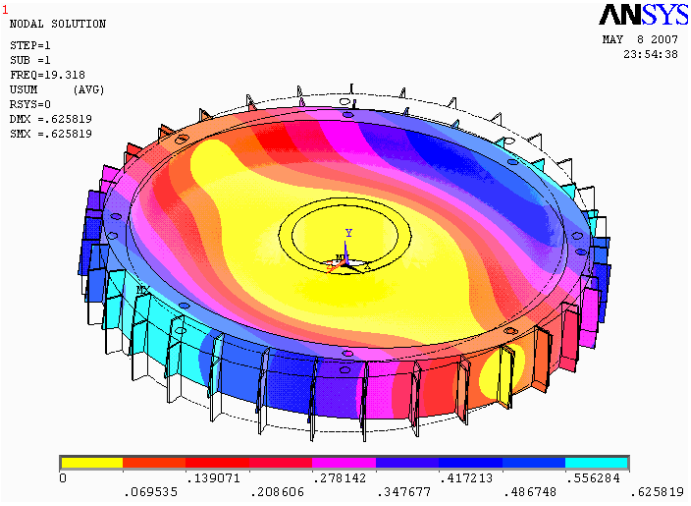


( a ) Mode i shape

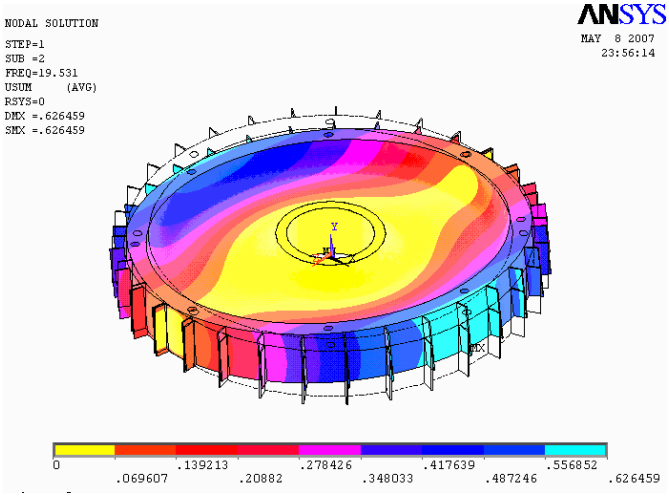


( b ) Mode ii shape

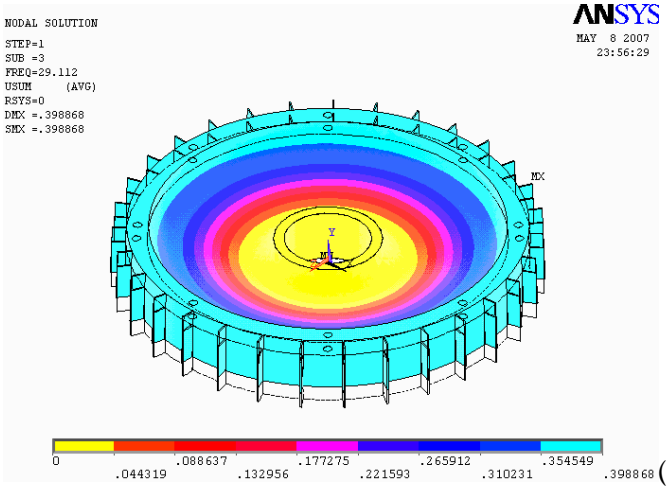


( c ) Mode iii shape

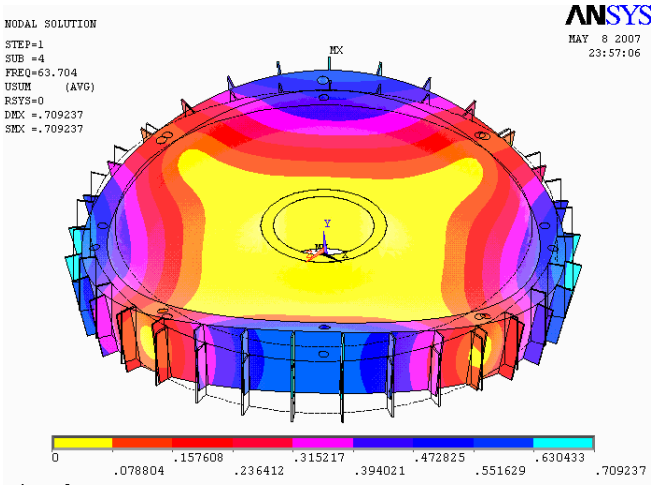


( d ) Mode iv shape

Figure 6.1 Mode shapes of rotating disk without crack.

Also, further study on mode shapes in modal analysis shows that as the natural frequency values keeps increasing, the modal diameters of the models are increased. Consequently, results obtained for the rotating disk without crack is used as reference for understanding the behavioral and physical change of a rotating disks with crack.

The distribution of natural frequencies for rotating disks with different circumferential crack is seen in graph[2] of figure 6.2 related with natural frequencies of the rotating disk without crack. As it can be seen from the graph, natural frequency values for rotating disk with crack had a different magnitude at each step when they compared with the natural frequency of the rotating disk without crack.

[2] For better description, line distributions for natural frequency have been scaled. Thus, to determine the exact values at each step, listed scaling factor should be used.

It is been discussed that softening of component due to existence of crack on system leads to change of the vibration characteristic of the component. Thus, the reason for change in natural frequencies between the rotating disk without and with crack can be stated as a change in stiffness of the disk due to crack formation and propagation i.e. due to disk softening. This conclusion is supported by the research made by Fredrick D. Ju on "Structural Dynamic Theory in Health Monitoring" ,[ 1 ].Note that from many possible natural frequencies for the rotating disk, only ten natural frequency values are expanded (extracted) in modal analysis.

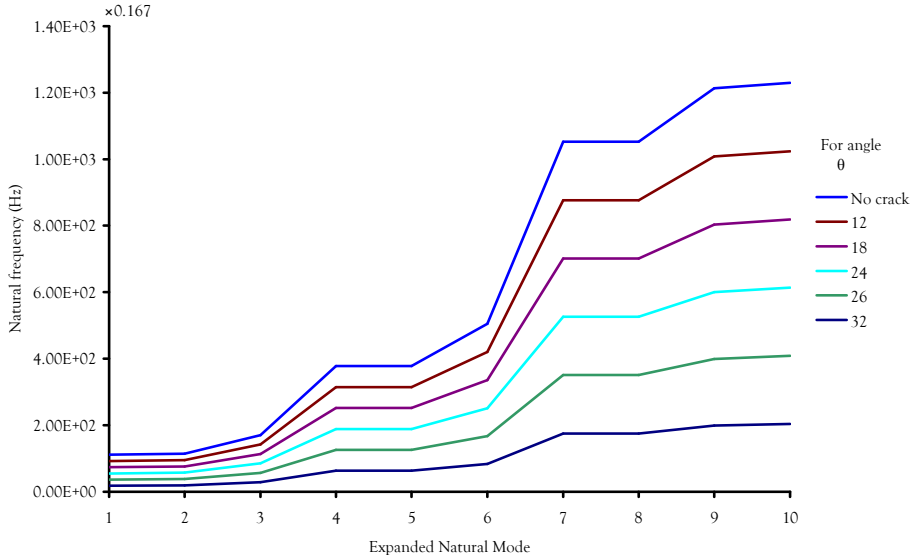


Figure 6.2 Natural frequency distributions for rotating disk with circumferentially oriented cracks as related with rotating disk without crack.

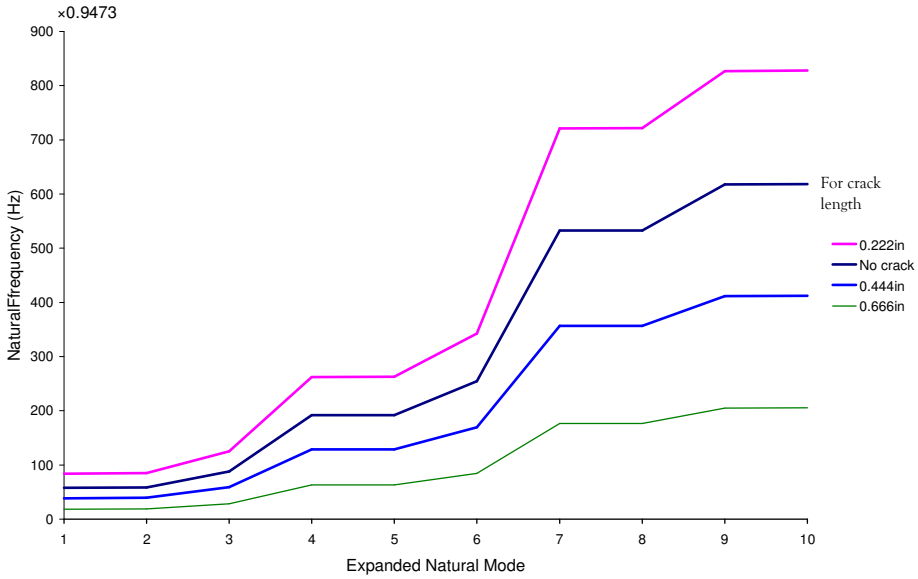


Figure 6.3 Natural frequency value distributions for rotating disk with radically oriented cracks as related with rotating disk without crack.

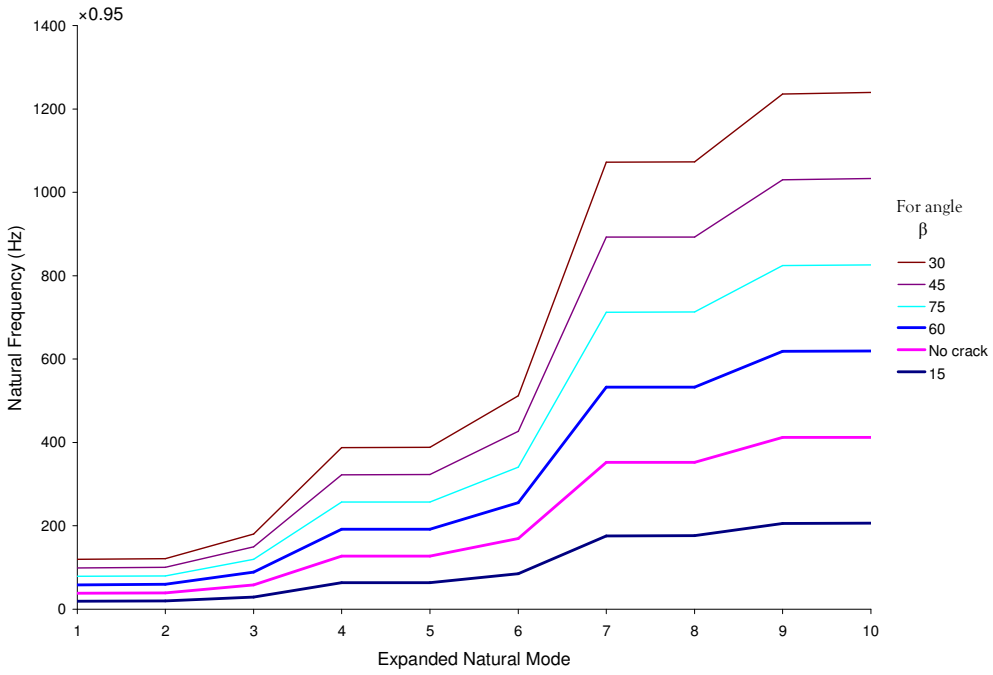


Figure 6.4 Natural frequency value distributions for rotating disk with arbitrarily oriented cracks as related with rotating disk without crack.

A behavioral change in natural frequencies for model with radially and arbitrarily oriented crack is observed in figure 6.3 and 6.4 graphs when they related with natural frequency value for model without crack. The same reason, which is softening of the component for minimized stiffness leads for change in natural frequency.

The change in natural frequencies between models with different orientation and length of crack is observed as compared with the natural frequency of model without crack in figure 6.2 - 6.4 graphs. The mode shapes of the models with different crack orientation and length is different when it compared with mode shape of a model without crack have a difference in their global and local shape (i.e. shape around crack). When we give attention to the first mode shape of the disk without crack, with circumferential crack, radial crack and an arbitrarily oriented crack, we can observe a global change in their shapes and magnitudes, figure 6.5. Regarding changes in localized mode shape, figure 6.6 and figure 6.7 clearly illustrate with the third and ninth mode shape of the models and we can relate them with mode shape of rotating disk without crack.

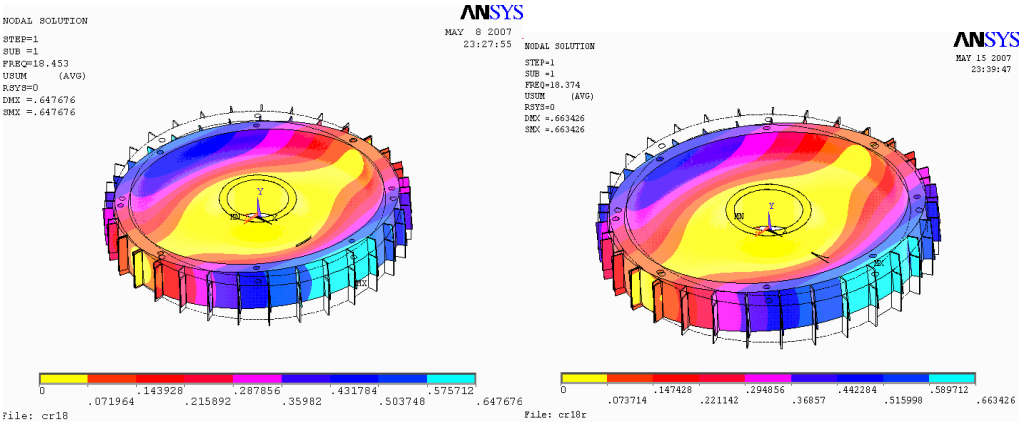


( a ) ( b )

( c )

Figure 6.5 The first mode shape rotating disk with circumferentially, radial crack& arbitrarily oriented cracks respectively.

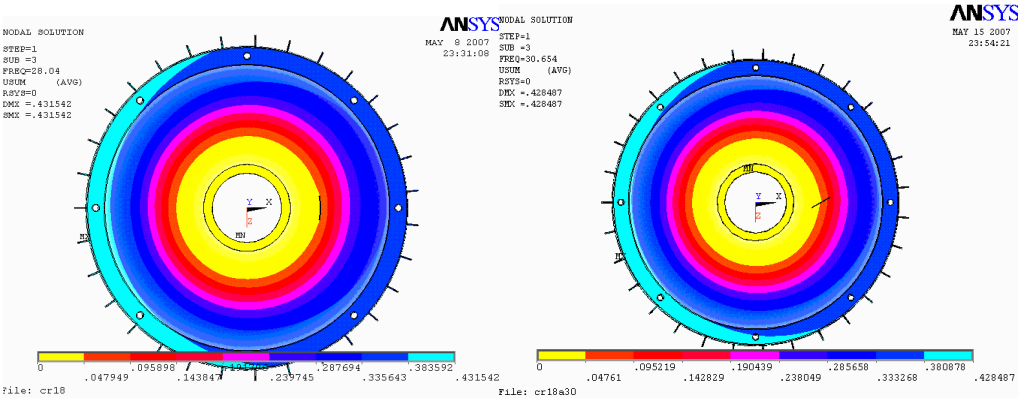


( a ) circumferentially oriented crack ( b ) arbitrarily oriented crack

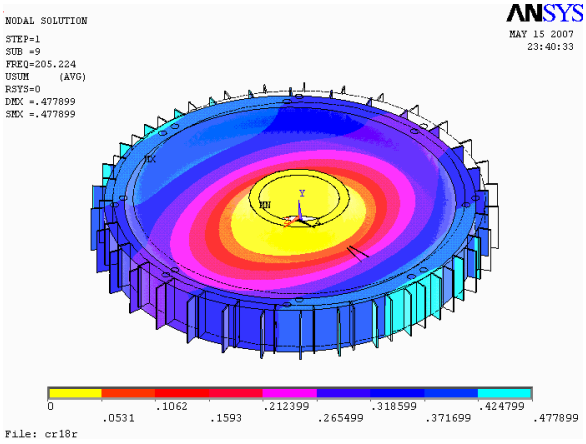


( c ) radially oriented crack

Figure 6.6 The local mode shape change in model due to crack 18 in its 3rd mode shape

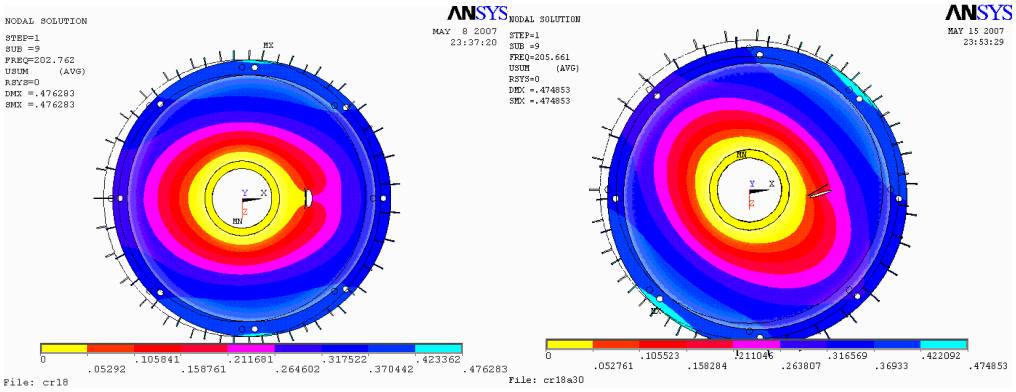


( a ) circumferentially oriented crack ( b ) arbitrarily oriented crack

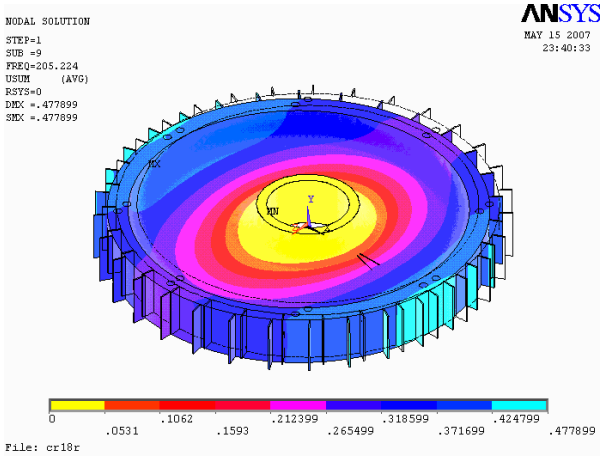


( c ) radially oriented crack

Figure 6.7 The local mode shape change in model due to crack 18 on its 9th mode shape

In addition to the modal analysis of the finite element model, analysis for distribution of deformation and stress due to inertia load are carried on the finite element model by ANSYS. Figure 6.8 ( a ) – ( b ) shows the distribution of the deformation and stress on rotating disk without crack at an angular rotation of 6000rpm respectively.

As is can be seen in the figures 6.8, the inertia load due to angular rotation on model made a uniform distribution for deformation and stress along its curved boundary of the rotating disk. The distribution of deformation keeps increasing form the middle region of the model to the outer radius of the model. While, for the predefined boundary condition the distribution of stress on the model is seen to be higher at the web section of the disk as related with other part of the model.

Consequently, since these regions are a sever position for a possibility of crack formulation due to fatigue load and it propagation on the disk. The stress distribution result is used to position the crack models at these regions taking into account the previous discussion and for a better result on deformation and stress magnitudes. Thus, the distribution of deformation and stress on the rotating disk without crack helps further analysis on crack behavior when it exists on rotating disk.

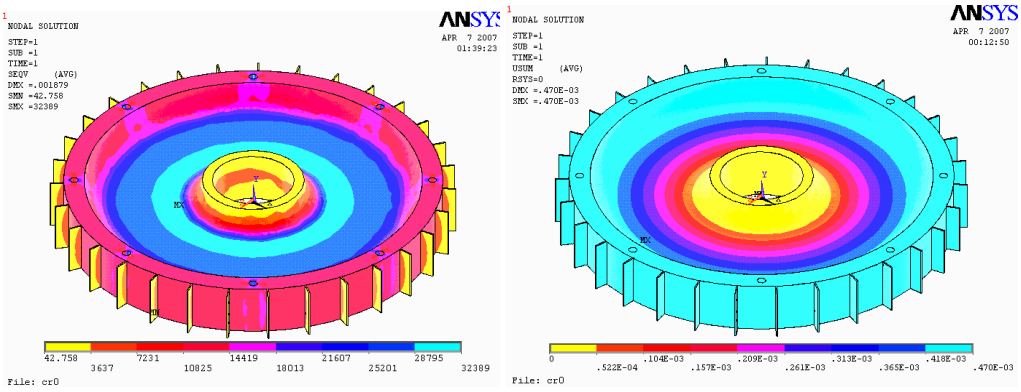


( a ) ( b )

Figure 6.8 Distribution of von Mises stress and deformation for rotating disk without crack, respectively.

The physical changes in the rotating disks when they exposed to crack have been observed by the distribution of in deformation using graph of figure 6.9 – figure 6.11. The graphs shows the relation of maximum deformation values of the rotating disks

for the range of angular rotation. Each graphs illustrate, the deformation magnitude of the rotating disks are increased when the angular speed increased.

Hence, as it is been discussed in Dynamics Theory when the angular speed in the system increased, system will be exposed to much more inertia loading. Thus, the system will be strained more which as a result higher deformation magnitude will be obtained on the system. Moreover, when we compared the magnitude deformation between rotating disk that exposed to circumferential and radial crack, results shows that models with circumferentially oriented crack leads to maximum deformation as compared with that of models exposed to radial cracks. The line of action of the inertia load that is perpendicular to crack opening direction for a circumferential crack can be considered as a reason.

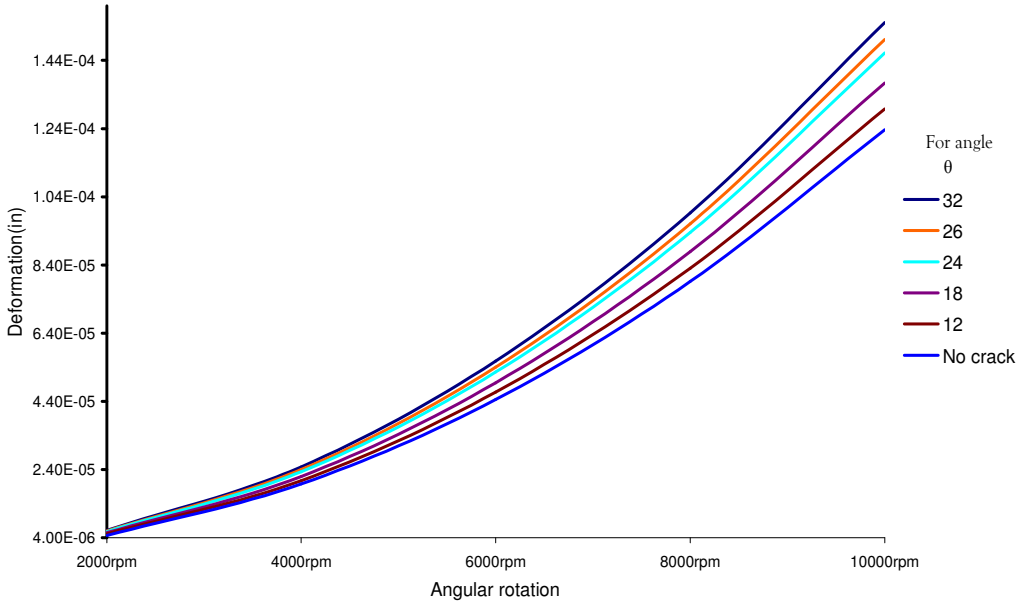


Figure 6.9 Distribution of deformation vector sum for rotating disk due to circumferentially oriented cracks.

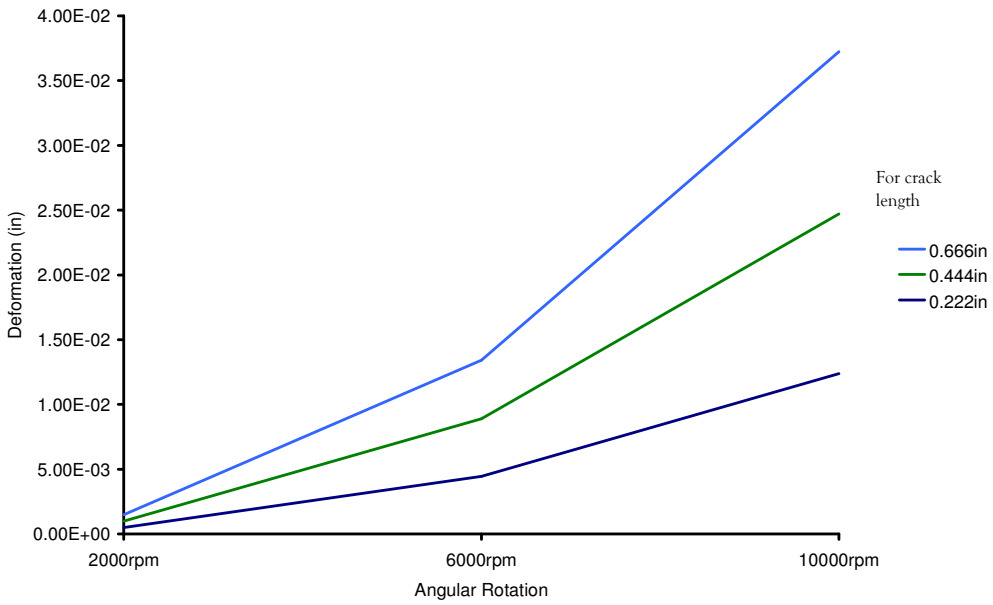


Figure 6.10 Distribution of deformation vector sum for rotating disk due to radically oriented cracks.

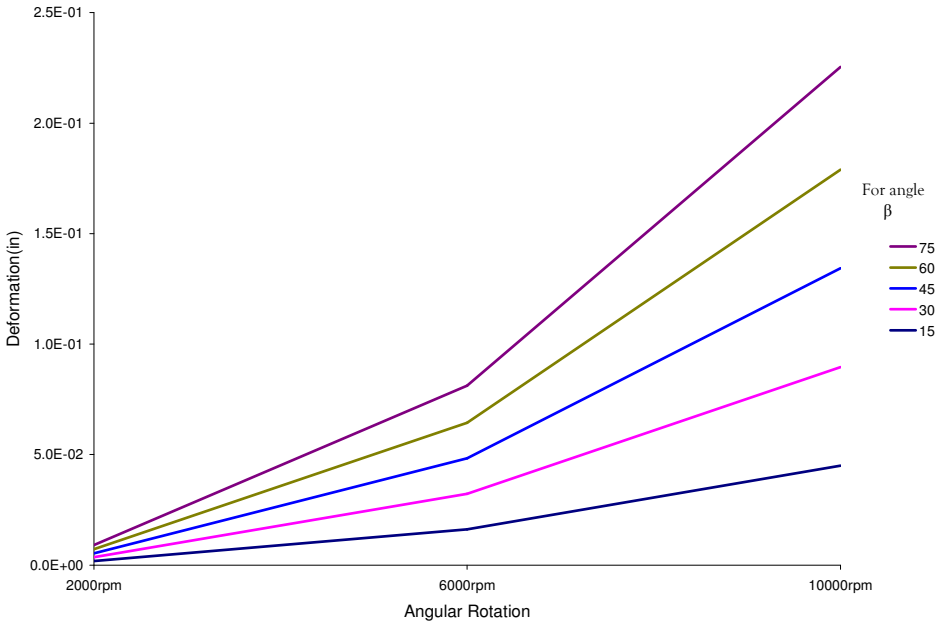


**Figure 6.11** Distribution of deformation vector sum for rotating disk due to arbitrarily oriented crack.

And, graphs of figure 6.12 – figure 6.14 illustrates the net change in deformation due to crack on the models. A change in deformation value on models has a direct relation to the change in angular rotation on the models verses angular speed. The net deformation value is obtained from the difference between the maximum

deformation value if rotating disks with crack and with out crack. This physical change through the models, when the rotating disk is exposed to crack is confirmed by research conducted by NASA research center, [ 18 ].

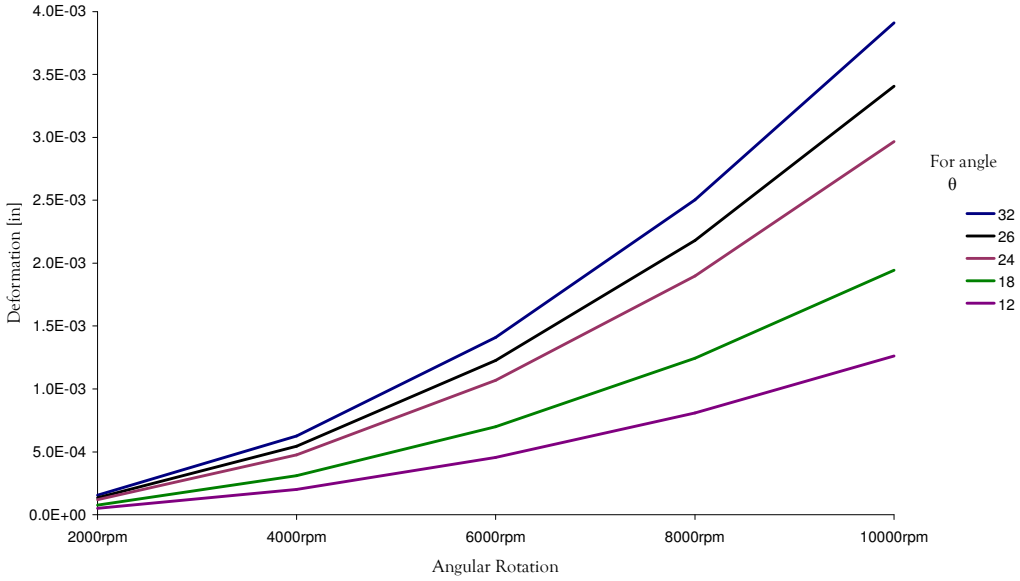


Figure 6.12 The net deformation value distribution for rotating disk due to the circumferentially oriented cracks.

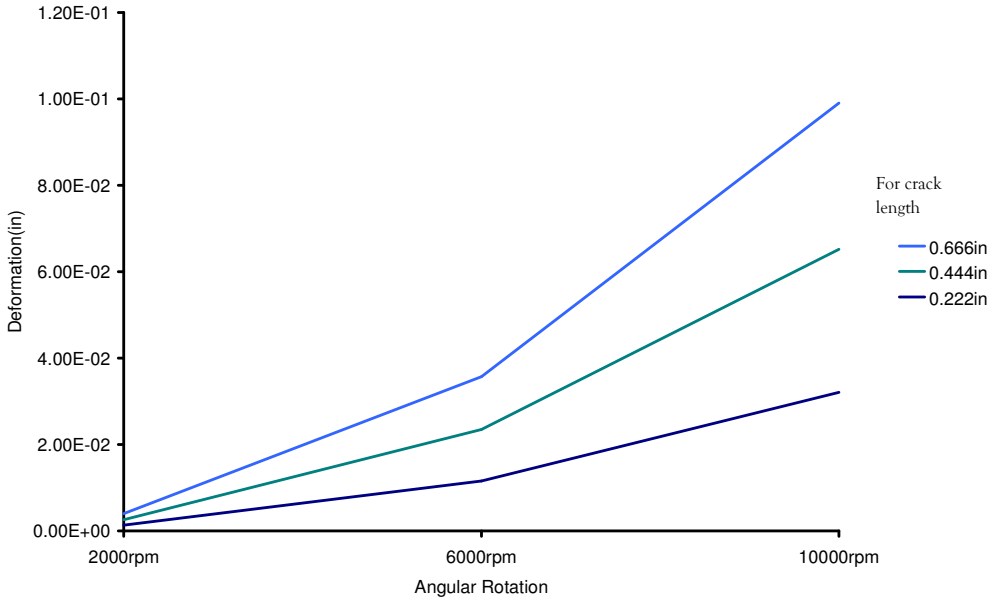


Figure 6.13 The net deformation value distribution for rotating disk due to the arbitrary cracks.

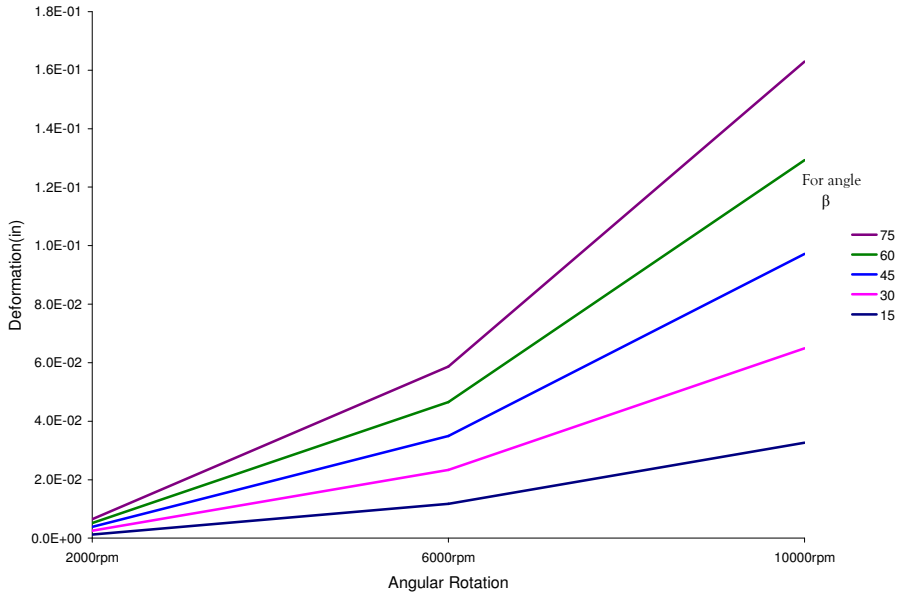


Figure 6.14 The net deformation value distribution for rotating disk due to the arbitrary oriented cracks.

In the above graphs, we observe the change in deformation value for rotating disk when models exposed to different crack length and orientation. In addition, as it can be seen from figure 6.15 the global and local distribution of deformation for models is influenced by crack length and orientation when the models exposed to crack. Figure 6.15 ( a ) - ( c ) illustrates a circumferential crack made significant change of deformation not only in global boundary of the models but also to around the cracks regions of the models. This localized crack effect is clearly described with an increased crack length i.e. a subtended angle of 12°, 18° and 32° in those figures. Besides, a localized deformation change is clearly illustrated in figure 6.17, where a crack changes it position from slight angle difference 15° from radial axis to high angle range equal to 75°.

Distribution of deformation for rotating disk with radial crack is illustrated by figure 6.16. As it can be seen, the existence of crack on the rotating disk significantly affects the global distribution of deformation when we compare it with rotating disk without crack. Moreover, further study on rotating disks with different radial crack length shows the same result. However we have to note this statement is made only in relation with limited input parameters that been used for analysis.

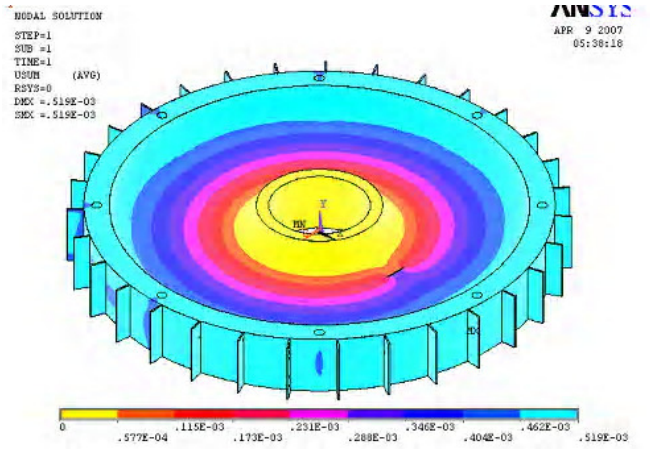


( a ) For crack angle equal to 12°

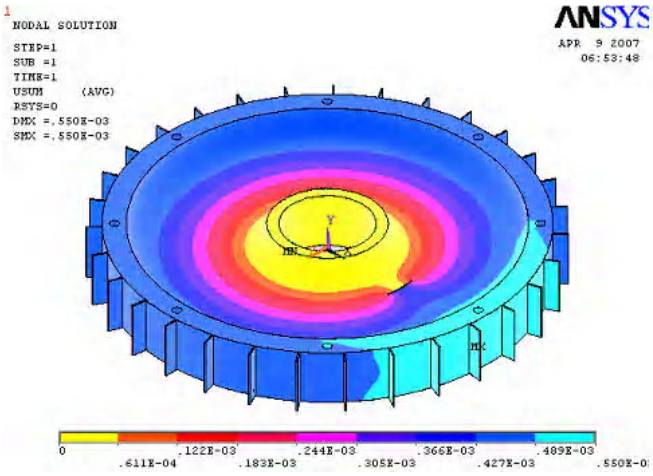


( b ) For crack angle equal to 18°

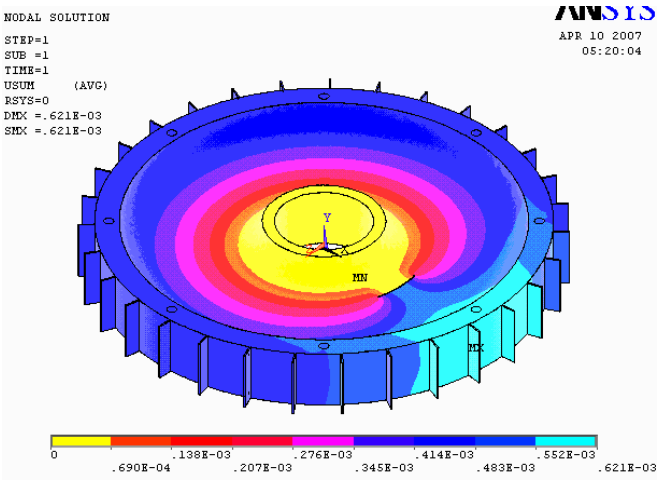


( c ) For crack angle equal to 32°

Figure 6.15 The distribution of deformation for rotating disk due to the circumferentially oriented crack.

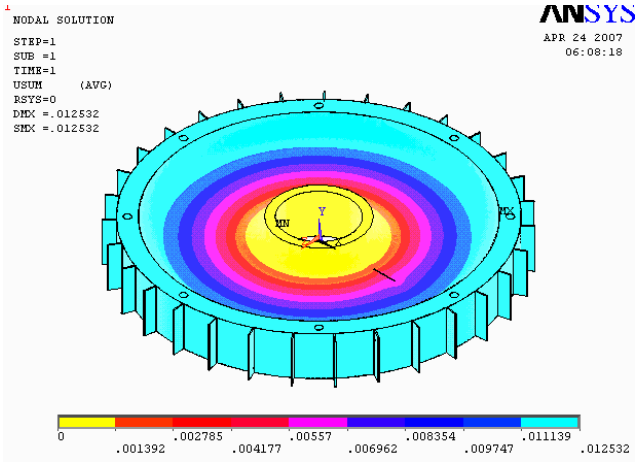


Figure 6.16 The distribution of deformation for rotating disk due to the radial oriented crack.[ crack including angle equal 18°]

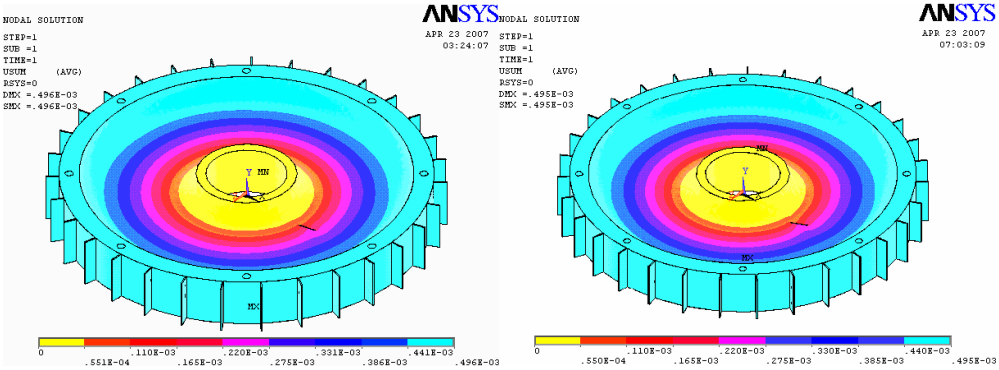


( a ) β = 15°　　( b ) β = 30°

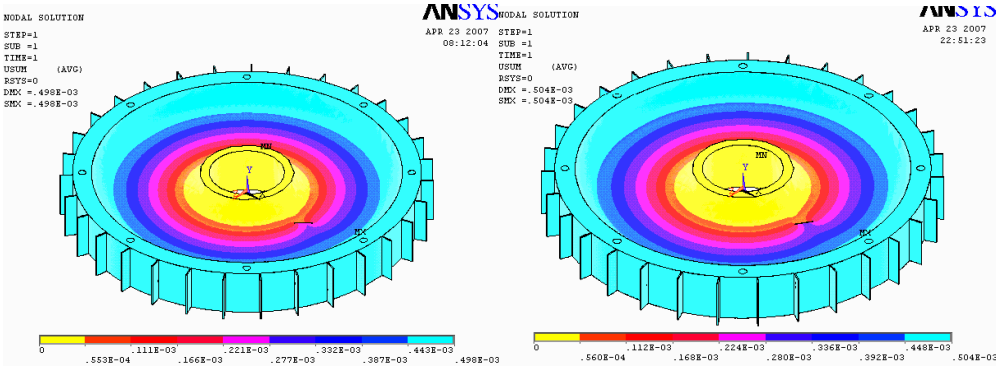


( c ) β = 45°　　( d ) β = 60°

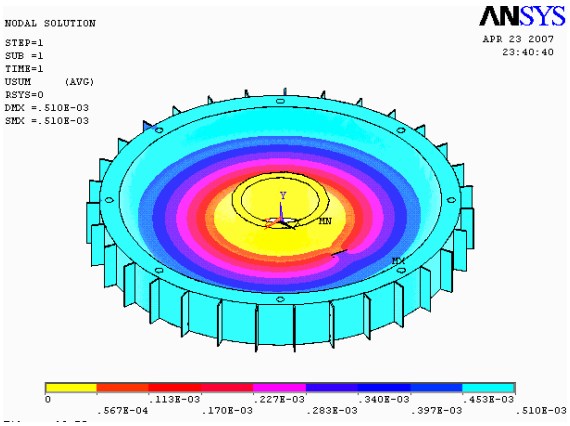


( f ) $\beta = 75^{o}$

Figure 6.17 Deformation distribution for rotating disk with arbitrarily oriented cracks.

From the stress analysis using ANSYS, stress distribution observed to be altered by existence of crack on the rotating disks when it is compared with rotating disk without crack. figure 6.18 - 6.19 clearly illustrate the magnitudes and distribution of the stress through out the models. It can be observed from the results that, crack tip surfaces are the region where disk is maximally stressed as compared with other region of the rotating disks. This is clearly seen from figure 6.18 b and 6.19 b, that the distribution of stress became more sever at crack tip regions. Thus, these regions with maximum stress had a possibility of crack growth as compared with other regions in the models.

Although, figures 6.18 and 6.19 shows that, the relative global stress distribution through out the models seems to be significant affected by existence of a radial crack. However, result of models with circumferential crack shows that, the attainable maximum stress through the model is much higher than models with radial crack. Thus, figure 6.20 shows the flow stress distribution change in the rotating disk when it is exposed to crack which orientation change from radial direction with different angle $\beta$.

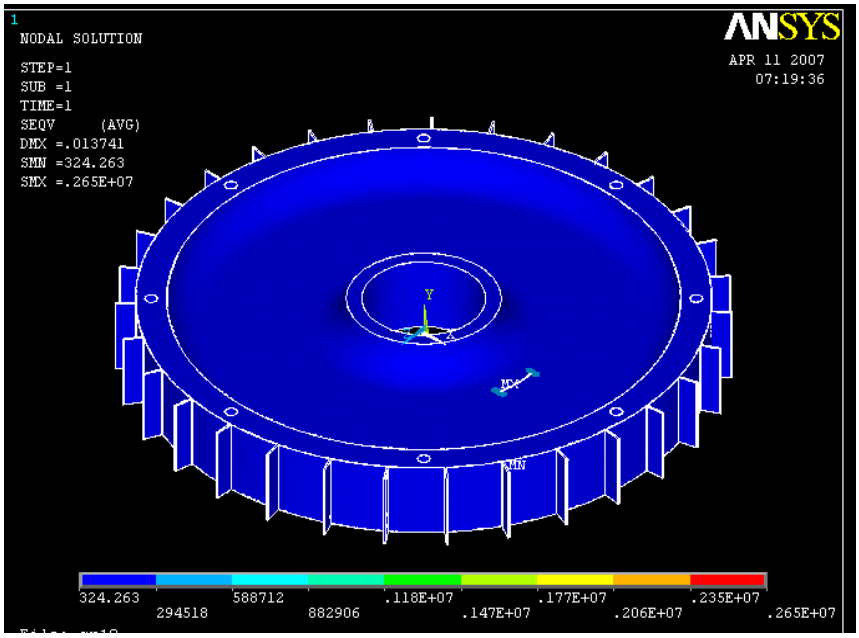


( a ) The stress distribution for rotating disk with circumferentially oriented crack.

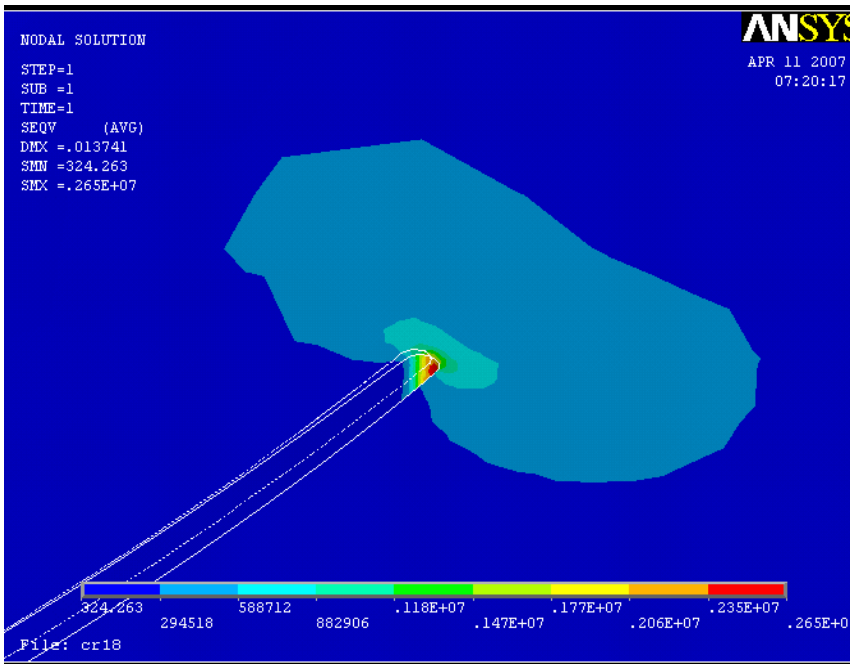


( b ) Stress around crack tip of a circumferential crack.

Figure 6.18 The stress distribution for rotating disk with circumferential crack.

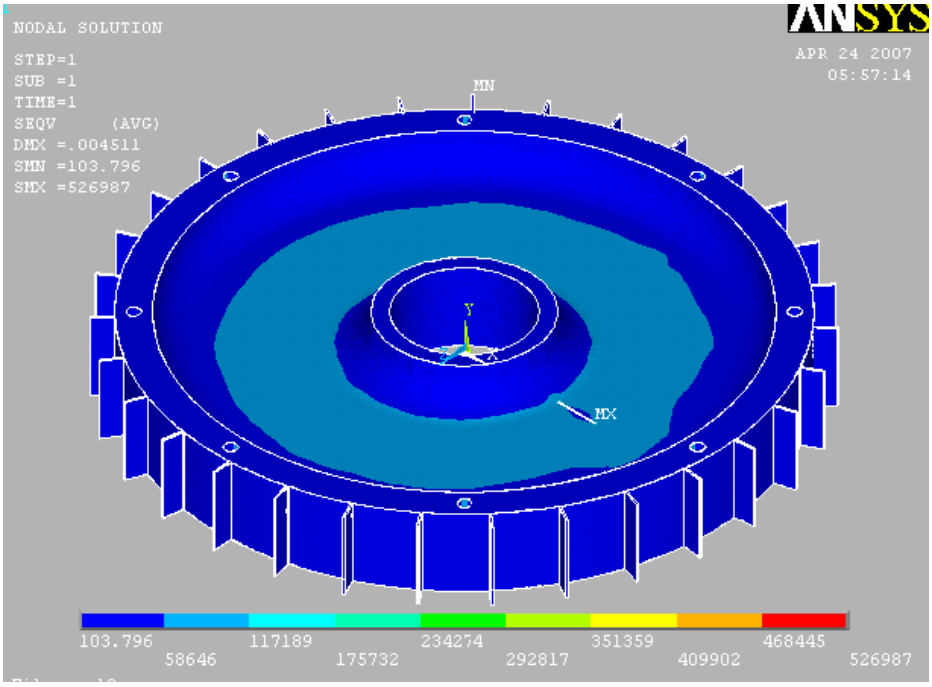


( a ) The stress distribution for rotating disk with radically oriented crack

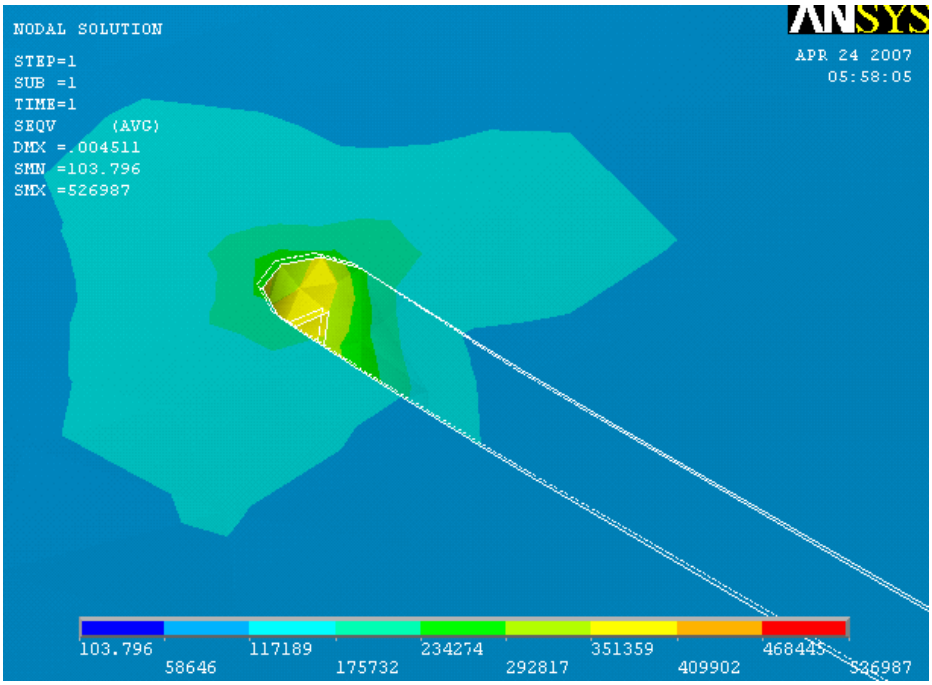


( b ) Stress around crack tip of a radial crack.

Figure 6.19 The stress distribution for rotating disk with radial crack.

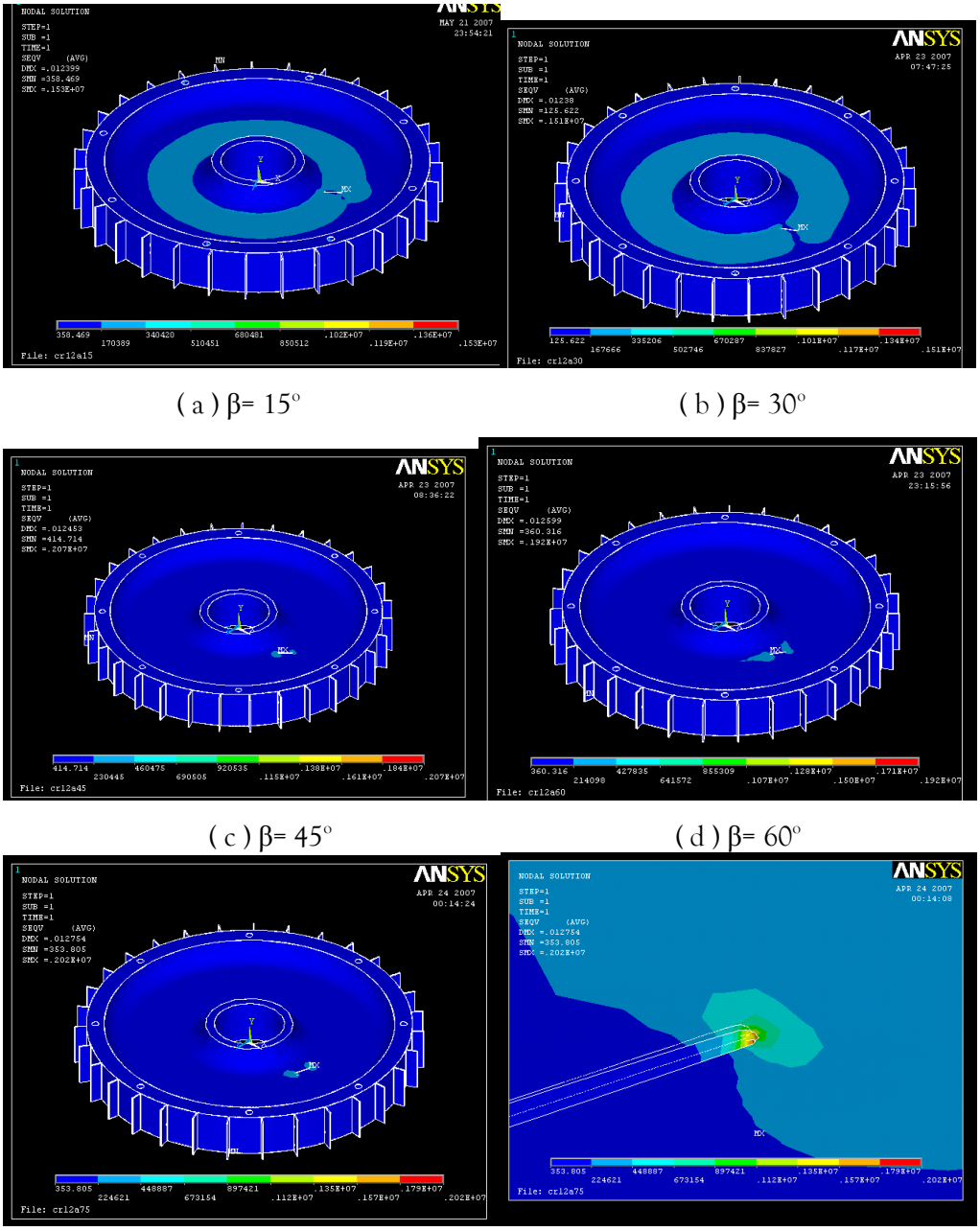


( a ) β= 15° ( b ) β= 30°

( c ) β= 45° ( d ) β= 60°

( e ) β= 75° ( f ) Stress around crack tip of a radial crack

Figure 6.20 The stress distribution for rotating disk with arbitrarily oriented crack.

Further, analysis for stress distribution on a rotating disk with crack length of 0.444in at different angle orientation i.e. at 15°, 30°, 45°, 60°, 75°, 90° had been done on finite element analysis software ANSYS. The result of the analysis shows that, the maximum stress developed on the rotating disk is when the crack is oriented at 45°

from radial axis. Besides, graph of figure 6.14 illustrates the relationship between the maximum stresses developed with crack angles at different orientations on the rotating disk. A range of angular rotation and a crack length of 0.444in are used as input parameters for stress analysis.

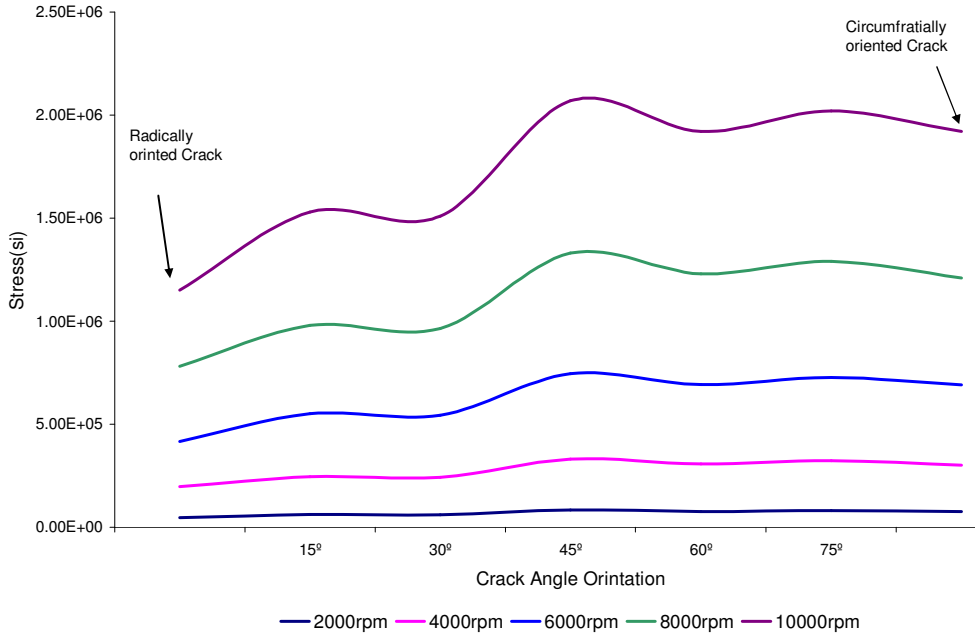


Figure 6.21 Von-Mises Stress relation with angular rotation and orientation of crack.

In addition, from the graph of figure 6.21, it is observed for selected angular rotation, the rotating disk is maximally stressed if it is exposed to a crack with its angular orientation of 45° from the radial axis. That is because, a region around a crack tips that orientation at 45° had a lesser energy strain so as to resist load as related with other regions of the disk. And, ends points of the lines shows the value of stress for rotating disk when it is exposed to radial crack and circumferentially cracks. Thus, their relative magnitude shows that, a rotating disk which exposed to circumferential crack is more severe than a rotating disk with a radial crack.

# Chapter Seven

## 7 Conclusion and Recommendation

### 7.1 Conclusion

In this thesis, the main objective is to find parameters that can be used for detection of a crack on rotating disk. First, the mathematical and numerical relations which represent the governing equation of the rotating disk are formulated by simulating the rotating disk by a structural member using "plate" theories. For modeling different crack types on the rotating disk fracture theories are applied. Then, finite element analysis software "ANSYS" is used for analysis on geometric models that simulate the physical component of rotating disk without and with crack. Taking in to account what it has been found from literature and results from this thesis study, the conclusions that we reached with are discussed below.

As the results of the modal analysis confirm, the natural frequency values of a rotating disk with crack has different magnitudes when it compared to those of a rotating disk without crack. Thus, natural frequency can be used as one parameter for identifying crack on the rotating disk.

The other parameter that can be used for identifying a crack in a rotating disk is mode shapes of the model. As per the result of the modal analysis, models of rotating disk that are exposed to crack have different mode shapes when we compare them with those of the rotating disk without crack. Further, the changes of mode shape between models without and with crack are not only along the global boundary of model but also in the local regions of crack surfaces. Consequently, this localized alteration of mode shape can be considered as an advantages for identifying crack not only to indicate that model is exposed to crack but also to identify the particular crack regions where crack formed among the total volume of the model.

In addition, we observe from the distribution of deformation that models of rotating disk with crack shows increase in the magnitude of deformation as compared with deformation of rotating disk without crack. Therefore, increment in magnitude of

deformation for real rotating disk from deformation magnitude of real rotating disk without due to other loading condition can be used as an indicator for the disk to identifying presence of crack. That is because the difference in magnitude owes to the existence of crack on model.

Thus, the natural frequency, the mode shape and deformation magnitude of a model can be used as means of identifying crack existence on models. Thus, we can use these indicators as parameters for detection of crack on rotating disk.

## 7.2 Recommendation for Further Research

Crack detection has been a very important issue to engineering sectors for minimizing catastrophic failure as well as for maintenance cost. In order to improve the effectiveness of current technology, the following research areas are recommended for future studies.

- ✓ In this thesis, cracks have been positioned only to the region where a rotating disk without crack stressed highly due to inertia load. However, there is a possibility of crack formation and propagation in other regions of the rotating disk. Thus, further research can be done by positioning the crack in other regions of the rotating disk by observing their relevance to crack formation and propagation, such as at tip of holes surface of the rotating disk. In addition to this, research can be done by modeling surface crack on rotating disk to find the behavioral change of the rotating disk if it contains such crack models.

- ✓ Only softening of disk due to crack formation is considered in the study of the behavioral change of the rotating disk in this thesis. Beside, taking into account that pre-stressing loads and joint condition between blade and rotating disk that can alter stiffness of the component can also be consider to as a source of softening effect. Therefore, further work can be done by applying a combination of those softening effect for finding the behavioral change of the rotating disk.

- ✓ To support the detection of crack on rotating disk by finding other parameters that can be used for monitoring crack formation and propagation. For example, analysis on the shift of center of mass of the rotating disk due to crack formation and propagation can applied.

- ✓ Taking into consideration that some real rotating disk operates under thermal loading in addition to inertia load as an external load, further research can made on rotating disk taking into account both loading conditions.

Finally, it is recommended that experimental research can be performed for conforming the analytical analysis result obtained. This thesis is limited to analytical analysis due to limitation of experimental setup for doing experimental investigation.

**Reference**


1. D. J.Fredrik, "Structural Dynamic Theory in Health monitoring" , *Vibration, Shock, Damage and Identification of Mechanical System*, ASME De-64, /1993/.
2. T. L. Anderson, *Fracture Mechanics*, 3ed, CRC Press LLC, 2005.
3. W. J. MaGonnajle, *Non-destructive Testing*, 2ed, Gordennad Breach, New York, 1969.
4. Decher and Weilend, "Neural-Net Based Optical NDE Method for Structural Health Monitoring", *Gleen Research Center* ,NASA, 2003-212492.
5. B. Li, X. F. Chen, J. X. Ma and Z. j. He, "Detection of Crack Location and size in Structures using Wavelet Finite Element Methods", *Journal of sound and vibration*, ELSEVIER, 285(2005)767-782.
6. D. Panteliou, G. Chondros, C. Argyrakis and D. Dimarogonas, "Damping Factor as an Indicator of Crack Severity, " *Journal of Sound and Vibration",* 241(2), (2001) 235-245.
7. D. Liu, "Damage Detection in Mechanical Structures through Coupled Response Measurements: A literature review" , dissertation, Australia, 2004.
8. C. Jintai, N. Chol and M. Jang ,"A Study on Free Vibration of a Spinning Disk" , *Journal of KSME* , 10 (2) 138-145, 1996.
9. J. Chung , E. Oh and H. Yoo, "Non-Linear Vibration of a Flexible Spinning Disc with Angular Acceleration" *Journal of Sound and Vibration* 231(2), (2000), 375-391.
10. J. W. Heo and J. Chung, "Vibration Analysis of a Flexible Rotating Disk with Angular Misalignment" *Journal of Sound and Vibration* 274 (2004) 821–841.
11. T. Tomioka "Analysis of free vibration of rotating Disk-blade coupled system by using Artifical springs and Orhogonal polynomial" *Journal of Sound and Vibration* 191, 1 (1996)53-73.
12. C. Wen-hwa and L. Ta-chyan, "A Mixed-Mode Crack Analysis Of Rotating Disk Finite Element Method" *Engineering Fracture Mechanics Note*, 18 (1) ,(1983) 133-143.
13. P. Rooke and J. Tweed, "The Stress Intensity Factors of a Radial Crack in a Finite Rotating Elastic Disc" *International Journal of Engineering Science*, 10 (1972) 709-714.

14. I. Makoto, "Rotating Disk Containing an Internal Crack located at an Arbitrary Position", *Engineering Fracture Mechanics Note*, 14 (1981) 549-555.
15. J.M. Lorenzo and D.J. Cartwright, "Boundary Element Weight Function Analysis of a Strip Yield Crack in a Rotating disk" *Theoretical and Applied Fracture Mechanics Note*, 21 (1994) 241-250.
16. H. Xin, F. George, H. Roland and F. Jerry, "Vibration Analysis and Health Monitoring of Cracks in Composite Disk Rotor Systems", *International Mechanical Engineering Congress and Exposition*, ASME, November, 2005.
17. G. Itzhak and C. Cody, "Crack Detection In A Rotating Dynamic System By Vibration Monitoring" part- 1 analysis, *Journal of Engineering for Gas Turbines and Power*, ASEM, 127(2005)425-434.
18. A.L. Gyekenyesi , J. T. Sawicki and G.Y. Baaklini, "Vibration Based Crack Detection in a Rotating Disk" Part1- Analytical Study, NASA, 2003.
19. Wayne C. Haase and Michel J. Drurnm, "Detection, Discrimination and real-Time Tracking of Cracks in rotating Disks: Patent Pending" *IEEE* (2002).
20. A.P.Boresi, R.J.Schmidt, O.M.Sidebottom, *Advanced Mechanics of Material*, 5th , John Wiley & Sons, Inc, USA, 1993.
21. H. Bo-Wun and K. Jao-Hwa, "Variation in the Stability of A Rotating Blade Disk with A Local Crack Defect", *Journal of Sound and Vibration 294 (2006) 486–502*.
22. D. P. Rooke and J. Tweed, "The Stress Intensity Factors of a Radial Crack in a Finite Rotating Elastic Disk", *Inr. J. Engng Sci.,10 (1972) 709-714*.
23. H. Goldstein, *Classical Mechanics*, 2nd. Addison-wesley publishing company, Inc., Philippines, 1980.
24. L. Jean, *Handbook of Material Behavior Models, Part II Failure of Material*, Academic press, USA, 2001.
25. T.L.Anderson, *Fracture Mechanics*, 2nd, CRC Press LLC.,1995.
26. O. C. Zienkiewicz, *The Finite Element Method*, 3ed , McGraw-Hill Book Company Ltd., 1977.
27. V. H. David, *Fundamentals of Finite Element Analysis*, McGraw-Hill Companies, 2004.
28. C. S. Krisnamoorthy, *Finite Element Analysis*, 2nd (1994), Tata McGrew Hill, New Delhi.

29. A. C. Ralph, *Vibration Monitoring and Diagnosis, Techniques for Cost-effective Plant Maintenance*, Halsted Press, USA, 1979.
30. R.J.Sanford, *Principles of Fracture Mechanics*, Peason Education, Inc, New Jersey, 2003.
31. H. C. Stephen, C. k. Deen, F. K. Edward and D. C. Pridemore-Brown, *Dynamics of Mechanical and Electro-mechanical system*, Robert E. Kieger Publisher Company, Inc., USA,1982.
32. M. P. Richard , *Dynamics of Machinery*, McGrew-Hill, Inc., 1967.
33. D. Childs, *Turbomachineary Rotordynamics, Phenomena, Modeling & Analysis*, John Wiley & Sons, Inc. USA, 1993.
34. S. S. Rao, *The Finite Element Method in Engineering*, 3rd , Butter Worth-Heine Mann, USA, 1999.
35. ASME, Structural Dynamic Aspect of Bladed Disk Assemblies, USA, 1976.
36. B. Suffork, Vibration in Rotating Disk Machinery, Proceeding of the institution of Mechanical Engineering, Waveney print services Ltd., 1992.
37. N.K. Bairagi , *A Text Book of Plate Analysis*, Wtanna Publishers, Delhi, 2003.
38. V. E. Saouma, *Fracture Mechanics, Lecture Note,* University of Colorado, Boulder, 2000.

# Acknowledgment

First of all, I would like to thank the almighty God; all things are happened because of him.

I would like to express my warmest thank-you to my Advisor Dr. Alem Bazezew for his continual guidance and supportive encouragement during the research. And, I would like to thank all teaching staffs and my class colleagues in mechanical engineering department for the assistance they provided at all levels of the thesis work.

A special thanks goes to my close friends Ato Taddese Diga, Ato Yimesker Siraw and Ato Achamyelew Aemro and for been with me all time when I need supporting materials for this thesis.

Last, but not least, I would like to thank my parents, my sister and brothers for supporting and encouraging during my stay in postgraduate study.